

## Response to referee 1

We are very grateful to referee 1 for the careful reading of our manuscript and for providing constructive comments which helped to improve the manuscript. This document includes all the referee's comments as well as our replies to every one of them.

### General comment from the referee

This manuscript shows some very nice measurements of temperatures in the stratosphere. The measurements compare well with various other sources. While I have several suggestions, I have no major recommendations for changes. My most serious complaint is that, while many of the authors of this manuscript speak excellent English, much of the text is very poorly written. I certainly do not think that it should be the reviewer's role to assist in this task, especially when several of the co-authors are completely capable of doing so.

#### **Author's response:**

We appreciate the positive feedback from the reviewer. Regarding the English writing we have made a detailed review of the text and it has been substantially improved in the new revised manuscript.

### Specific comments

#### **1. Comments from the referee:**

Page 5 – “Radiosondes reach an altitude of 35km”. This, and later statements, gives the impression that all radiosondes from Payerne reach precisely this altitude, but I am skeptical that this is the case.

#### **Author's response:**

We agree with the referee that in the way that the sentence was written sounds that RS always reach that altitude, which is certainly not true. In fact, the target altitude of RS is 10 hPa (~32 km), but many go a bit higher, as high as 35 km. For this reason, we have rephrased the sentence in the way that can be read below.

#### **Author's changes in the manuscript:** p. 5, line 9

“The target level of radiosondes is 10 hPa (approx.. 32 km), and hence cover only the lower stratosphere.”

**2. Comments from the referee:** Figure 3 – Given that, according for Figure 4d, the measurement response falls to well below 50% at ~17km, and that, as far as I have been able to determine, other TEMPERA studies show sensitivity only up to at best ~7km, suggesting that TEMPERA measures into the upper troposphere is very deceptive. It does certainly not, as the text suggests “cover the full troposphere and stratosphere”.

**Author's response:**

We agree with the referee that the measurement response of TEMPERA is not high enough in the full range from ground to the stratopause. For this reason, we have updated Fig. 3 showing that TEMPERA does not cover the upper troposphere and the lower stratosphere. We have also slightly modified the sentence indicated by the referee in order to be more precise.

**Author's changes in the manuscript:** p. 6, line 8

“As we can see TEMPERA is the only instrument that is able to cover almost the full troposphere and stratosphere.”

**3. Comments from the referee:** Figure 4b - This Figure is a simplification of a very similar Figure 14 in Stähli et al. (2013). In that figure it is stated that “In the center of the lines we use all channels and on the wings of the line we use a binning of 3 channels for data reduction”. I am almost certain that this is why the middle channels are noisier, and that this has nothing to do with the Zeeman effect, as is stated in the paper.

**Author's response:**

We thank the referee for this clarification. We agree with the referee that most of the noise observed for the residuals in the central part of the lines comes from different binning used. The Zeeman effect could be responsible of some differences between the measured spectra and the modelled ones (the model does not include Zeeman effect), but the differences should be smaller than the ones observed in this Figure. We have clarified this point in the manuscript in the way that can be read below.

**Author's changes in the manuscript:** p. 8, lines 12-15

“The larger differences observed in the center of the emission lines (see Fig. 4b) is mainly due to a different binning used in the center of the lines and on the wings of the lines (Stähli et al., 2013). In addition, the Zeeman effect could explain some small differences in the center of the lines since it is not incorporated in the forward model (Navas-Guzmán et al. 2015).”

**4. Comments from the referee:** Figure 4c - What is meant by “observation error”? Given that there are systematic changes  $>2K$  in the dataset, I assume that this must be some kind of random error estimate. If this is the case please label it as such. How is it calculated?

**Author's response:**

The observation error is the error of the retrieved profile due to measurement noise, i.e. the random error. It is calculated by propagating the measurement uncertainty (the measurement noise) through the retrieval using Gaussian error propagation.

**Author's changes in the manuscript:** p. 8, line 23

“Finally, the total, observational (random error due to measurement noise) and smoothing errors are also calculated with this method and are shown in Fig. 4e.”

**5. Comments from the referee:** Figure 6 - Given the very large discrepancy between the MLS and other measurements on 4 February above 35 km, this clearly warrants some discussion. It is very troubling that neither the LIDAR nor the MWR show the decrease in temperature above 35km. Do nearby (in time and space) MLS profiles show the same structure? Do the authors think that this is a bad MLS profile?

**Author's response:**

We have double-checked that the nearby (in time and space) MLS profiles also show the same structure than the one presented in the Figure 6a. Since this structure is not detected by the other instruments (TEMPERA and lidar) we think that these could be problematic MLS inversions. Anyway, the idea of presenting this figure in the manuscript was just to show the different altitude ranges and spatial resolutions of the instrumentation used in our study. The observed differences between instruments in these three individual cases evidence the importance of our statistical analysis to really characterize the performance of the different instruments.

**6. Comments from the referee:** Page 9 - "The measurements presented in the plot show the importance of continuous observations for a fixed location, since the variability of atmospheric parameters such as temperature evinces the necessity of measurements with good temporal resolution." This suggests that there are temperature variations every few hours (a conclusion that can certainly not be reached by looking at Figure 5). If this is the case, please show such. If not, then certainly daily satellite measurements must be adequate, and this statement should be removed.

**Author's response:**

According to the referee's suggestion we have added a new plot to Figure 5 in order to show the high variability that temperature can have in the stratosphere in the course of few hours. In this new plot (Fig 5, right), three individual profiles on 3 January 2015 are presented. Differences of up to 15 K are observed between the first profiles (at 03:00 UTC) and the third one (at 13:00 UTC) confirming our previous statement. We have modified the text in the manuscript in order to mention these results in the way that can be read below.

**Author's changes in the manuscript:** p. 9, lines 5-9

"Figure 5 (right) shows an example of strong variation of temperature in the stratosphere for a winter day (3 January 2015). In this case, the temperature changed up to 15 K for some altitudes in the course of only 10 hours. These measurements show the importance of continuous observations for a fixed location, since the important variations in temperature observed cannot be captured by only occasional measurements or measurements with poor temperature resolutions."

**7. Comments from the referee:** Page 11 - It is stated that, above 35km the RS profiles were extrapolated using TEMPERA profiles. But the top altitude of RS profiles varies, so exactly what does this mean? Were only RS profiles which reached 35km included. If there was data above this was it included (instead of using the TEMPERA data)?

**Author's response:**

What we did was to interpolate each individual RS profile to the altitude grid of TEMPERA, and then fill the existing gap between each individual RS profile and TEMPERA profile (RSs usually do not reach altitudes higher than 35) with TEMPERA measurements in order to use the averaging kernels of TEMPERA in the convolution of the RS profiles. In order to clarify this point, we have modified the statement of page 11 in the way that can be below.

**Author's changes in the manuscript:** p. 11, line 6-8

“The RS profiles were interpolated to the altitude grid of TEMPERA radiometer, and completed in the upper part with the TEMPERA measurements, since RSs usually do not reach altitudes higher than 30-35 km. Afterwards, the profiles were convolved using the averaging kernels of TEMPERA.”

**8. Comments from the referee:** Figures 7, 9, and 12 – The most piece of information on these is the comparison between TEMPERA and the convolved retrievals from the other instruments. Since this is the case, it would be best to plot the interpolated line first, and then the convolved and TEMPERA lines on top of this. As the plots are currently shown it is sometimes difficult to tell whether the TEMPERA line coincides with the convolved or the interpolated measurement. Alternatively, the interpolated measurement could even be dropped from these plots.

**Author's response:**

According to the referee's suggestion we have updated these three figures (Fig. 7, 9 and 12). In the new plots a better visualisation of the most interested lines (the convolved profiles from the different instruments and from TEMPERA) can be observed.

**9. Comments from the referee:** Figures 7 and 9 – is the black deviation line TEMPERA vs. RS interp or RS conv? In fact, throughout much of the text it is not clear whether convolved or unconvolved RS and/or MLS data is being used.

**Author's response:**

All the comparisons between TEMPERA and the different datasets have been carried out using the convolved profiles of the latter. This point has been indicated for each comparison. However, in order to make clearer for Fig. 7 as the referee suggest we have explicitly indicated it in the description of this figure. The sentence reads as is indicated below.

**Author's changes in the manuscript:** p. 11, line 12

“The temperature deviations along this period between TEMPERA and the convolved measurements from RS are shown in the lower panels (black lines).”

**10. Comments from the referee:** The step in the data shown in Figure 7 very helpful in that it provides a useful measure of the systematic errors in these retrievals. I applaud the investigators for not homogenizing the data between the two periods.

**Author's response:**

We appreciate the positive feedback from the reviewer.

**11. Comments from the referee:** Page 13 – “near time-coincident”. Does this mean that the MLS profile was taken during the period of spectral integration for the TEMPERA measurement? If so, please state this. If not, please state what exactly “near time coincident” means. The same applies to the RS comparisons.

**Author's response:**

Yes, as the referee indicated “near time-coincident” in our study means that the MLS and RS profiles were taken during the period of the spectral integration for the TEMPERA measurements. It has been clarified in the manuscript as can be read below.

In the case of RS it was already indicated in the manuscript (page 10, line 20): “The TEMPERA profiles closest in time to the RS launch have been selected in order to do this comparison.”

**Author's changes in the manuscript:** p. 13, line 15

“The data were also restricted to cases with near time-coincident between TEMPERA and MLS, which means that the MLS profiles were taken during the period of the spectral integration for the TEMPERA measurements.”

**12. Comments from the referee:** Page 15 and Figure 11 – The authors note that: “the bias and the standard deviation observed between MLS and RS is very similar to the values observed in the comparison between TEMPERA and RS in period 2.” If do not know, and it seems to be nowhere stated, whether in Figures 8 and 10, the MLS and RS measurements are convolved before comparison with the MWR. If they are (and I think they should be), then the appropriate comparison in Figure 11 would be convolved MLS with convolved RS profiles. This could be added as a dashed line in Figure 11.

**Author's response:**

In Figure 11 we just evaluated the agreement between MLS and RS data in the range where both measurements are comparable. We did not convolve these profiles with the AVK of TEMPERA in order not affect the comparison of these two instruments (RS and MLS) with a third one (TEMPERA). In addition, we have to keep in mind that the measurement response of TEMPERA below 20 km is low, so it would also limit the comparison between MLS and RS in the lower part. In addition, the results after the convolution would be affected by the repair of the attenuator in TEMPERA (since it also affects the AVK). For all these reasons and in order to make our statistics comparable with other studies (e.g., Schwartz et al., 2008) we just compared the profiles from both instruments without convolving them.

**13. Comments from the referee:** Figure 17 – The legend is a bit confusing. Please make the 4 instrument lines solid and thick enough so that one can distinguish lidar and

WACCM. Then separately show two styles of lines, one for Period 1 and one for Period 2.

**Author's response:**

We would like to point out that lidar measurements are only available above 29 km and that in this figure there is only a small range where the mean deviation for both instruments (lidar and WACCM) are almost identical (around 30 km). Below 29 km only the profile from WACCM is shown (blue line) so there is not any overlap with the one corresponding to the lidar (black line). Respect to the styles of the lines we are already representing different styles for both periods as the referee suggests: dashed lines for period 1 and solid line for period 2.

**14. Comments from the referee:** Table 1 – Since Period 1 and Period 2 are presented everywhere else, why is only Period 2 in this table?

**Author's response:**

The idea was to present in this table the values that can characterise better the accuracy and precision of TEMPERA radiometer. Since during the first period TEMPERA was operating with a defective attenuator we decided to show only the values corresponding to period 2 that is when the instrument was operating in optimal conditions.

# Intercomparison of stratospheric temperature profiles from a ground-based microwave radiometer with other techniques

Francisco Navas-Guzmán<sup>1</sup>, Niklaus Kämpfer<sup>1</sup>, Franziska Schranz<sup>1</sup>, Wolfgang Steinbrecht<sup>2</sup>, and Alexander Haefele<sup>3</sup>

<sup>1</sup>Institute of Applied Physics (IAP), University of Bern, Bern, Switzerland

<sup>2</sup>Meteorologisches Observatorium Hohenpeißenberg, Deutscher Wetterdienst, Hohenpeißenberg, Germany

<sup>3</sup>Federal Office of Meteorology and Climatology MeteoSwiss, Payerne, Switzerland

*Correspondence to:* Francisco Navas-Guzmán (francisco.navas@iap.unibe.ch)

## Abstract.

In this work the stratospheric performance of a relatively new microwave temperature radiometer (TEMPERA) has been evaluated. With this goal in mind, almost three years of temperature measurements (January ~~2015~~2014 - September 2016) from the TEMPERA radiometer were intercompared with ~~the measurements from different techniques~~ as simultaneous measurements  
5 from other techniques: radiosondes, MLS satellite and Rayleigh lidar. This intercomparison campaign was carried out at the aerological station of MeteoSwiss at Payerne (Switzerland). In addition, the temperature profiles from TEMPERA were used to validate the temperature outputs from the SD-WACCM model. The results showed in general a very good agreement between TEMPERA and the different instruments and the model with a high correlation (higher than 0.9) in the temperature evolution at different altitudes between TEMPERA and the different datasets. An annual pattern was observed in the stratospheric temper-  
10 ature with ~~in general~~ generally higher temperatures in summer than in winter and with a higher variability during wintertime. A clear change in the tendency of the temperature deviations was detected in summer 2015 which was due to the repair of an attenuator in the TEMPERA spectrometer. The mean and the standard deviations of the temperature ~~deviations~~ differences between TEMPERA and the different measurements were calculated for two periods (before and after the ~~reparation~~ repair) in order to quantify the accuracy and precision of this radiometer ~~along these almost three years~~ over the campaign period. The  
15 results showed absolute biases and standard deviations lower than 2 K for most of the altitudes ~~and~~. And comparisons proved the good performance of TEMPERA ~~to measure~~ in measuring the temperature in the stratosphere.

## 1 Introduction

The thermal structure of the atmosphere is one of the most important ~~atmospheric~~ characteristics for determining chemical, dynamical and radiative processes in the atmosphere. In the stratosphere, temperature can influence chemical processes, and its  
20 vertical profile is fundamental ~~for investigating~~ to investigations of other atmospheric species ~~as for example ozone or~~, such as ozone and water vapor (Haefele et al., 2009; Stähli et al., 2013; Moreira et al., 2015). In addition, stratospheric temperature is ~~also~~ a very important indicator of climate change (Randel et al., 2009). The temperature trends can provide evidence of the roles of natural and anthropogenic climate change mechanisms. Several studies have shown ~~a detectable~~ observed the observation of

a pattern of tropospheric warming and lower stratospheric cooling during the last few decades of the twentieth century which is very likely related to anthropogenic emissions of trace gases, ozone and aerosols (Ramaswamy and Schwarzkopf, 2002; Santer et al., 2006; Schwarzkopf and Ramaswamy, 2008; Randel et al., 2009; Bindoff et al., 2013).

Stratospheric temperatures can present a large variability ~~along the~~ in time, specially during winter. For example, the stratosphere can experience sudden temperature increases (Sudden Stratosphere Warming, SSW) due to dynamical processes where the temperature can change by several tens of degrees within a very short time (Flury et al., 2009; Scheiben et al., 2012). ~~These~~ Monitoring these fast changes require measurement techniques with high temporal and spatial resolution ~~in order to be able to monitor these processes in the stratosphere.~~

The in situ technique of radiosonde is extensively used for tropospheric temperature measurements due to its high vertical resolution. However, ~~in the stratosphere, they~~ radiosondes are only able to cover the lower part ~~, reaching maximum altitudes of the stratosphere, reaching a maximum altitude~~ of around 35 km. In addition, ~~they present also an important disadvantage against other techniques and it is their low temporal resolution since in the best of the cases they are only launch~~ since at best they are launched four times a day, they offer only a very low temporal resolution compared with other techniques.

At present, stratospheric temperature profiles are mostly obtained by ~~means of~~ remote sensing methods, such as lidars and microwave radiometers. Rayleigh lidars have been shown to be a powerful tool ~~to monitor the temperature for monitoring temperatures~~ in the middle atmosphere with a high spatial and temporal resolution (Hauchecorne and Chanin, 1980; Keckhut et al., 2001; Steinbrecht et al., 2009). However this technique's main drawback is that they ~~can not be operated either daytime~~ cannot be operated during daytime, or under cloudy or rainy conditions. ~~In this sense microwave~~ Microwave radiometer measurements can overcome these difficulties, since the measurements in the microwave region are almost ~~not affected~~ unaffected by liquid water and the radiometers can be continuously operated providing temperature profiles with a reasonably good spatial and temporal resolution. Most of the microwave radiometers for stratospheric temperature measurements are operated on board ~~of~~ satellites (e.g. MLS instrument on the Aura satellite as described in Waters et al. (2006), AMSU-A instrument on the Aqua satellite as described in Aumann et al. (2003) and the SABER instrument on the TIMED satellite as described in Remsberg et al. (2003)).

The possibility of using ground-based microwave radiometry for stratospheric temperature measurements was ~~shown for the first time~~ first shown in Waters (1973) and it has ~~been recently~~ recently been implemented (Shvetsov et al., 2010; Stähli et al., 2013). The technique is based on the stratospheric thermal emission from high-rotational ~~, magnetic dipole~~ transitions of molecular oxygen around 53 GHz. ~~Ground-based microwave radiometer measurements present as main advantages~~ The main advantages of ground-based radiometer measurements are that they can provide unattended continuous measurements of temperature profiles in almost all weather conditions with ~~a~~ reasonably good spatial and temporal resolution in the altitude range between 20 and 50 km above ~~see~~ sea level (asl). In addition, long-term measurements in a fixed location allow the local atmospheric thermodynamics to be characterized. In this study we are going to present almost three years of stratospheric temperature measurements from the TEMPerature RAdiometer (TEMPERA) which has been designed and built by the Institute of Applied Physics of the University of Bern (Switzerland). This is the first ground-based microwave radiometer that is able to retrieve temperature measurements in the troposphere and in the stratosphere at the same time. Tropospheric retrievals from



this radiometer have been evaluated in detail in other studies (Stähli et al., 2013; Navas-Guzmán et al., 2014, 2016). In this work we will focus on the stratospheric performance of TEMPERA (from 20 to 50 km) comparing its measurements with the ones from different instruments and techniques as: radiosondes, satellite and lidar measurements. In addition TEMPERA profiles will be used to validate the temperature outputs from SD-WACCM model.

The results obtained in this study provide a detailed evaluation of the temperature retrievals from the TEMPERA radiometer. The paper has been organized in the following way. The description of the different instrumentation used in this work is introduced in Section 2. Section 3 presents a detailed description of the methodology used for the microwave temperature retrievals. Section 4 presents the results of the different comparisons of RS, MLS satellite, lidar, SD-WACCM versus the TEMPERA radiometer. And finally, we conclude with a summary of the key findings in Section 5.

## 2 Experimental site and instrumentation

A special campaign has been set up at the aerological station in Payerne (46.82° N, 6.95° E; 491 m above sea level (asl), Switzerland) of the Swiss Federal Institute of Meteorology and Climatology (MeteoSwiss). For this campaign, the TEMPERA radiometer was moved from the ExWi building of the University of Bern (Bern, Switzerland) to Payerne in December 2013. The main goal of this campaign is to assess the tropospheric and stratospheric performance of TEMPERA using the versatile instrumentation available at this MeteoSwiss station (Navas-Guzmán et al., 2016). In particular, this study will focus on the intercomparison of the stratospheric temperature profiles from TEMPERA.

Next, we will introduce the ground-based microwave radiometer called TEMPERA and all the other instrumentation used in this study. As it was already mentioned, the TEMPERA radiometer is the first ground-based microwave radiometer which is able to measure temperature profiles in the troposphere and in the stratosphere simultaneously (Stähli et al., 2013; Navas-Guzmán et al., 2014, 2016). It measures the microwave emission of the molecular oxygen in the 51-57 GHz range. The instrument consists of a frontend to collect the microwave radiation and two backends for the spectral analysis (a filter bank and a Fast Fourier Transform spectrometer (FFT) spectrometer). The incoming radiation is directed into a corrugated horn antenna using an off-axis parabolic mirror. The antenna is characterized by a Half Power Beam Width (HPBW) of 4°. The detected signal in the two backends is calibrated by means of an ambient hot load in combination with a noise diode. The calibration of the noise diode is performed every month using a hot (ambient) and a cold (liquid nitrogen) load. Figure 1 (left) shows a picture of TEMPERA radiometer where its different components can be observed: mirror (1), microwave absorbers (hot(2) and cold (3) load), receiver (4) and styrofoam window (5). Figure 1 (right) shows the isolated room where TEMPERA is located at the aerological station of MeteoSwiss at MeteoSwiss aerological station in Payerne (Switzerland).

The tropospheric measurements by TEMPERA are performed by means of a filter bank. It covers a total of 12 frequencies uniformly distributed on the wing of the 60 GHz oxygen emission complex. Since tropospheric temperature measurements are not the topic of this study more details about technical aspects of the filter bank and the measurement protocol for this mode can be found in Stähli et al. (2013) and Navas-Guzmán et al. (2016).



**Figure 1.** The TEMPERA instrument at the MeteoSwiss Station in Payerne, Switzerland.

For stratospheric measurements a second backend is used. It consists of a digital FFT spectrometer (Acqiris AC240) which measures the two pressure-broadened oxygen emission lines centered at 52.5424 and 53.0669 GHz. The bandwidth of this spectrometer is 960 MHz and has a resolution of 30.5 kHz. The receiver noise temperature  $T_N$  is around 480 K. More technical details about the different components of the microwave receiver, such as the IQ-Mixer ~~or~~ and the local oscillator (LO), can be found in Stähli et al. (2013). An example of a calibrated spectrum (brightness temperature) measured with this spectrometer on 2 of February of 2014 is shown in Fig. 2.

A styrofoam window allows views of the atmosphere over a range of different elevation angles (from 20° to 60°). The ~~operation of the instrument radiometer is operated~~ inside a laboratory ~~presents as main advantage that the radiometer is protected primarily to protect it~~ against adverse weather conditions. The frontend ~~itself~~ has additional temperature stabilization ~~with using~~ Peltier elements in combination with a ventilation system ~~leading to a stabilization of that allows~~ the frontend plate ~~to be stabilized to~~ within  $\pm 0.2$  K (Stähli et al., 2013).

Every measurement cycle takes 1 minute ~~of duration~~ and starts with a calibration using the hot load in combination with a noise diode for 9 ~~seconds~~, followed by atmosphere measurements. These atmospheric measurements consist of ~~a~~ scanning from 20° to 60° elevation ~~angles~~ in steps of 5° (9 angles). The observations at all the angles are used for tropospheric measurements while only the observations at 60° elevation angle, which take 15 seconds, are used for stratospheric measurements (Stähli et al., 2013). Details about the methodology used to obtain stratospheric temperature profiles from these measurements will be given in section 3.

15 Independent in-situ temperature ~~measurement~~ measurements have been taken by means of radiosondes. They ~~are regularly~~ have been launched twice a day at the aerological station of Payerne since 1954. ~~Radiosondes reach an altitude of 35 km, covering in this way~~ The target level of radiosondes is 10 hPa (approx. 32 km), and hence cover only the lower stratosphere.

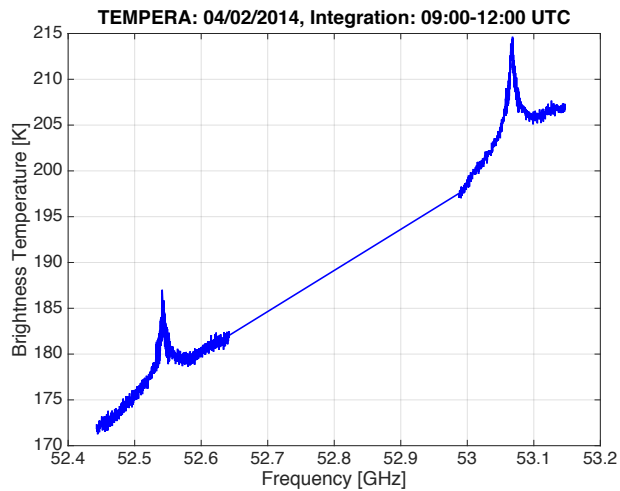


**Figure 2.** Spectrum of brightness temperatures measured with TEMPERA on 4 February 2014 from 09:00-12:00 (UTC). Only the FFT channels of the the first line at 52.5424 GHz and the second line at 53.0669 GHz used in the temperature retrievals are shown.

The ~~Their~~ spatial resolution ranges between 10 ~~to a maximum of~~ and 80 m with a highest resolution in the first seconds of the flight. The Swiss Radiosonde SRS-C34 introduced in 2011 uses a thermocouple for temperature measurements and a polymer  
 20 hygristor for relative humidity measurements. Pressure is calculated from temperature and GPS altitude assuming hydrostatic equilibrium. The achieved uncertainties are  $\pm 0.2$  K for temperature,  $\pm 2$  hPa ~~(accuracy 2 hPa)~~ (accuracy increases with height) for pressure and  $\pm 5$  to 10% for relative humidity.

Stratospheric temperature have been also obtained from the Microwave Limb Sounder (MLS) instrument on board of the  
 Aura satellite. MLS ~~makes has been making~~ measurements of atmospheric composition, temperature, humidity and cloud ice  
 25 in the upper troposphere, stratosphere and lower mesosphere since August 2004 (Waters et al., 2006). It observes thermal  
 microwave emission from Earth's limb viewing forward along the Aura spacecraft flight direction, scanning its view from the  
 ground to 90 km every 25 seconds. Aura is in a near-polar 705 km altitude orbit. As Earth rotates underneath it, the Aura  
 orbit stays fixed relative to the sun; to give daily global coverage with 15 orbits per day. Aura is part of NASA's A-train  
 group of Earth observing satellites. These satellites fly in formation with the different satellites making measurements within  
 30 a short time of each other. Temperature profiles are retrieved from MLS measurements using radiances near the O<sub>2</sub> spectral  
 bands at 118 GHz for the stratosphere and mesosphere and at 239 GHz for the troposphere (Yan et al., 2016) using the optimal  
 estimation theory (Rodgers, 2000). Four different versions of MLS data have been released to date. The initial version 1.5  
 (v1.5), was replaced by version 2.2/2.3 (v2) in 2007 and version 3.3/3.4 (v3) in 2010. The most recent production version,  
 version 4.2 (v4), replaced v3 in February 2015. All the MLS data presented in this study correspond to the ~~last~~ latest  
 35 (v4).

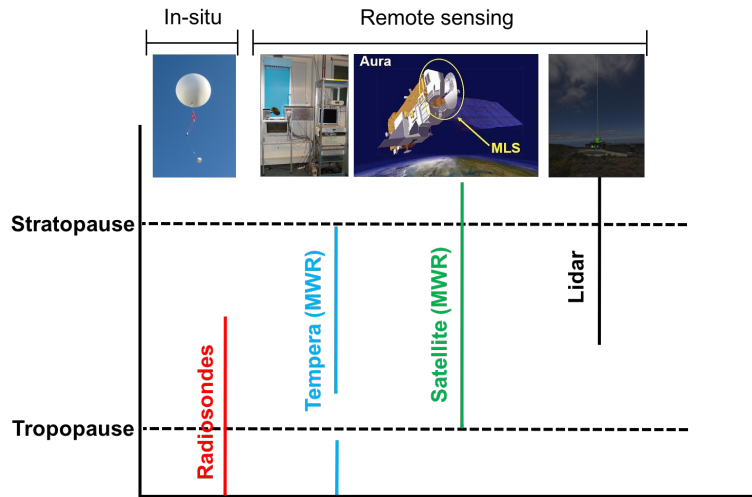


**Figure 3.** Measurement ~~range-ranges~~ for the different techniques used in this study (radiosondes, Tempera radiometer, MLS and lidar).

Temperature measurements in the upper stratosphere have been also obtained from a lidar at Hohenpeißenberg, Germany (47.8° N, 11.0° E). This lidar has been operated since September 1987 by the German Weather Service (DWD) and has provided one of the longer NDACC time series (Steinbrecht et al., 2009). It emits intense ultraviolet light pulses at 353 nm generated from a Xenon Chloride excimer laser and a Hydrogen Raman cell. Light intensity scattered back from air molecules in the atmosphere (by Rayleigh scattering) is recorded as a function of altitude (=time from pulse emission to reception of backscattered light). Above the stratospheric aerosol layer, that is above 25 to 30 km, the returned light intensity is proportional to air density. Assuming hydrostatic equilibrium, this (relative) density profile can be integrated downward over altitude, providing a (relative) pressure profile. Division of the (relative) pressure profile by the (relative) density profile then yields the temperature profile. See Hauchecorne and Chanin (1980) for details. The method requires an initial guess for temperature (or pressure) at the far end around 70 to 80 km altitude, but because of the large increase of pressure with decreasing altitude, this choice of initial value has virtually no influence on the derived temperatures below around 50 to 60 km altitude. The lidar requires clear nights for operation, and typically provides 80 to 90 nightly mean temperature profiles per year. Precision-The precision of the derived temperature is about  $\pm 0.5$  K at 30 km,  $\pm 1$  K at 45 km,  $\pm 5$  K at 60 km and  $\pm 10$  K at 70 km (all 1 sigma). Vertical resolution is about 1.5 km. The lidar derived temperature has a low-small bias of about 2 K between 30 and 50 km, which is not well understood. See Steinbrecht et al. (2009) for details.

Figure 3 shows the different ranges of measurements for of each instrument used in this study (radiosondes, TEMPERA radiometer, MLS satellite and lidar). As we can see TEMPERA is the only instruments which is able to cover almost the full troposphere and stratosphere.

### 3 Methodology

#### 3.1 Temperature profiles from TEMPERA radiometer

Oxygen is a well-mixed gas whose fractional concentration is independent of altitude below approx. 80 km, so the microwave radiation from it contains information primarily on atmospheric temperature. The retrievals of stratospheric temperature profiles from TEMPERA are based on the measurements of two oxygen emission lines centered at 52.54 and 53.06 GHz (see Fig. 2). The shape of these lines ~~are is~~ governed by a pressure broadening mechanism up to 60 km of altitude, therefore the measured spectra can provide vertical information. The wings of the emission lines provide information of the radiation coming from low altitudes (higher broadening caused by higher pressure) while the center of the lines give information of the radiation coming from upper altitudes (smaller broadening and lower pressure). Both emission lines measured by TEMPERA are used at the same time with a bandwidth of 200 MHz around the first line and of 160 MHz around the second ~~line~~. Only measurements at the ~~observational elevation angle of highest elevation angle (60° are taken)~~ are used for stratospheric measurements with the digital FFT spectrometer. ~~It implies that during a measurement cycle~~ This limits the integration time with the FFT spectrometer ~~is to 15 s in each minute measurement cycle~~. In order to get a low enough noise level the measurements are integrated for half an hour which requires two hours of measurement time, since only one quarter of the measurement time is ~~spent used~~ for the digital FFT spectrometer (Stähli et al., 2013). Therefore the time resolution of the stratospheric temperature profiles from the TEMPERA radiometer is two hours.

Obtaining temperature profiles from the calibrated brightness temperature spectrum ~~showed~~, an example of which is shown in Fig. 2, requires a solution ~~of to~~ the radiative transfer equation. ~~This is not unique and~~ A unique solution does not exist, ~~so~~ some statistical constraints are needed in order to obtain physically meaningful solutions. In our case we use the optimal estimation method (OEM) (Rodgers, 2000) by means of the radiative transfer model ARTS/QPack (Eriksson et al., 2011). The method is based on Bayes' probability theorem and ~~detailed description about it applied~~ a detailed description of its application to TEMPERA measurements can be found in Stähli et al. (2013).

The ARTS package implements the radiative transfer equation (forward model) ~~to simulate~~, simulating the brightness temperature as:

$$\mathbf{y} = F(\mathbf{x}, \mathbf{b}) + \epsilon \quad (1)$$

where ~~the~~ F denotes the forward model, the vector  $\mathbf{y}$  corresponds to the measured spectrum (brightness temperature),  $\mathbf{x}$  is the true temperature profile,  $\mathbf{b}$  contains some additional forward model parameters, and  $\epsilon$  is the measurement noise.

The solution to the inverse problem is ~~obtain~~ obtained by using the Gauss-Newton iterative method, whose solution can be expressed in a matrix notation as ~~follow~~ follows:

$$\mathbf{x}_{i+1} = \mathbf{x}_i + \left( \mathbf{S}_a^{-1} + \mathbf{K}_i^T \mathbf{S}_\epsilon^{-1} \mathbf{K}_i \right)^{-1} \left[ \mathbf{K}_i^T \mathbf{S}_\epsilon^{-1} (\mathbf{y} - F(\mathbf{x}_i)) - \mathbf{S}_a^{-1} (\mathbf{x}_i - \mathbf{x}_a) \right] \quad (2)$$

where the vector  $\mathbf{x}$  is the true temperature profile,  $\mathbf{y}$  is the measured spectrum (brightness temperature),  $\mathbf{x}_a$  is the a priori temperature profile,  $\mathbf{S}_a$  is the a priori covariance matrix and  $\mathbf{S}_e$  is the observation error-covariance matrix. The use of the forward model is ~~noted~~ denoted by  $F_x$  and the vector  $\mathbf{K}$  is the weighting function ( $\mathbf{K} = \partial F / \partial \mathbf{x}$ ).

An important tool used very often in the OEM is the averaging kernel matrix  $\mathbf{A}$  (Rodgers, 2000). This matrix describes the response of the retrieved temperature profile  $\hat{\mathbf{x}}$  to the true temperature profile  $\mathbf{x}$  and is defined as:

$$5 \quad \mathbf{A} = \mathbf{D}_y \mathbf{K}_x = \frac{\partial \hat{\mathbf{x}}}{\partial \mathbf{x}} \quad (3)$$

where  $\mathbf{K}_x$  is the weighting function ~~matrix defined before~~ already defined, and  $\mathbf{D}_y = \partial F / \partial \mathbf{x}$  is the ~~so-called~~ so-called contribution function.

The rows of  $\mathbf{A}$  are called the averaging kernels (AVK) and they ~~describes~~ describe the sensitivity of the retrieval for a certain height level to a perturbation at other levels. The sum of the AVK is called the measurement response (MR), which describes the contribution of ~~measurement~~ measurements to the retrieved profile at a certain height.

The method needs an a priori temperature profile in order to constrain the solutions to physically meaningful results. As a priori profiles, monthly mean temperature profiles from radiosonde ~~measuremens~~ measurements at Payerne from 1994 to 2011 are used in the lower part (ground to 15 km) and mean MLS temperature profiles from a climatology are used in the upper part. As ~~apriori~~ a priori covariance matrix  $\mathbf{S}_a$  a function decreasing exponentially with a correlation of 3 km is used assuming a standard deviation of 2 K. For the observation errors the residuals of the inversion are considered (difference between the integrated spectra and the fit of the spectra). Under regular conditions these errors range between 0.5 and 1.5 K (Stähli et al., 2013).

In the radiative transfer calculations ( ~~$F(x, b)$~~   $F(\mathbf{x}, \mathbf{b})$ ) the absorption coefficients of the different species are calculated using different models: Rosenkranz (1998) for  $H_2O$ , Rosenkranz (1993) for  $O_2$  and Liebe et al. (1993) for  $N_2$ . The density profiles of oxygen ( $O_2$ ) and nitrogen ( $N_2$ ) are incorporated by ARTS assuming standard atmospheric profiles for summer and winter (Anderson et al., 1986). In the case of tropospheric water ~~vapour~~ vapor a profile with an exponential decrease is considered. This profile is calculated with the measured surface water vapor density from a weather station and assuming a scale height of 2000 m (Bleisch et al., 2011).

Figure 4 shows an example of temperature inversion from TEMPERA measurements using ~~OEM~~ the OEM result obtained on 1 October 2015 for the time interval from 22 to 00 UTC. In Fig. 4a we can observe that the forward model brightness temperatures (red lines) agree well with the measured brightness temperatures (black lines) ~~excepting~~ except for around the line center. The larger differences observed in the center of the emission lines (see Fig. 4b) ~~can be due to the Zeeman effect that~~ is mainly due to a different binning used in the center of the lines and on the wings of the lines (Stähli et al., 2013). In addition, the Zeeman effect could explain some small differences in the center of the lines since it is not incorporated in these ~~retrievals~~ (Stähli et al., 2013; Navas-Guzmán et al., 2015) the forward model (Navas-Guzmán et al., 2015). Fig. 4c presents the a priori temperature profile used in the inversion (black ~~dash~~ dash-dashed line) and the retrieved temperature profile (blue line). Figure 4d shows the averaging kernels (black lines), the measurement response (red line) and the height resolution, which is defined as the full-width at half-maximum (FWHM) of the averaging kernels (blue line). We can observe that for this inversion

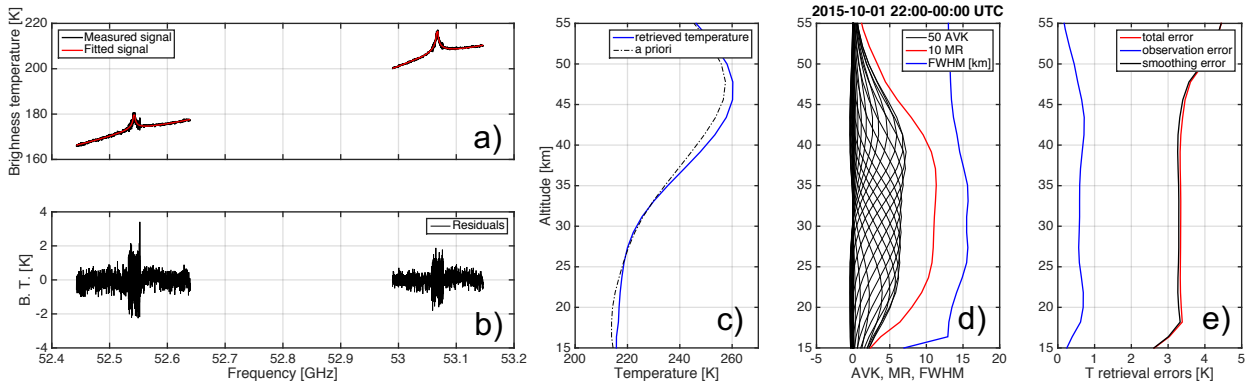


**Figure 4.** Temperature retrieval of 1 October 2015 using [the optimal estimation method \(OEM\)](#). a) Brightness temperature measured with TEMPERA (black lines) compared with the forward model brightness temperature (red lines) obtained for this retrieval. b) Residuals for this inversion. c) Retrieved temperature and a priori profile. d) Averaging kernels, measurement response and FWHM [km] are plotted. e) Temperature retrieval errors.

the height resolution ranges between 13 and 16 km. The MR shows values larger than 0.8 in the range between 20 and 43 km, meaning that 80% of the contribution to the retrieved temperature profile comes from the measurements. These values decrease with altitude reaching 0.5 at 47 km for this case. We would like to point out that the altitude range of the stratospheric temperatures from [the TEMPERA radiometer](#) used in this study correspond to levels with a high MR (higher than 0.8 [in-at](#) most of the [altitudes altitudes](#)). Finally, the total, observational ([random error due to measurement noise](#)) and smoothing errors are also calculated with this method and are shown in Fig. 4e.

5 In order to compare the temperature profiles from the different instruments ([radiosondes RS](#), MLS satellite, lidar) and also from the WACCM model with the ones from TEMPERA radiometer the profiles are [firstly-first](#) interpolated to the pressure grid of TEMPERA [and after that they are convolved using, and then are convolved with](#) the averaging kernel of this radiometer in order to take into account the different height [resolution resolutions](#). Equation 4 gives the expression [to calculate for calculating](#) the convolved temperature profiles:

$$10 \hat{\mathbf{x}}_r = \mathbf{x}_a + \mathbf{A} (\mathbf{x}_r - \mathbf{x}_a) \quad (4)$$

where  $\mathbf{x}_a$  is the a priori profile of the radiometer,  $\mathbf{A}$  is the averaging kernel and  $\mathbf{x}_r$  is the interpolated reference profile.

#### 4 Results: Evaluation of stratospheric temperature profiles from TEMPERA

[The TEMPERA radiometer](#) has been almost continuously measuring since 2014 at the aerological station of MeteoSwiss at Payerne (Switzerland). Figure 5 ([left](#)) shows the stratospheric temperature evolution obtained from TEMPERA for [almost](#) [these-the almost](#) three years of measurements. From this plot a clear annual pattern can be observed with [in-general-generally](#)

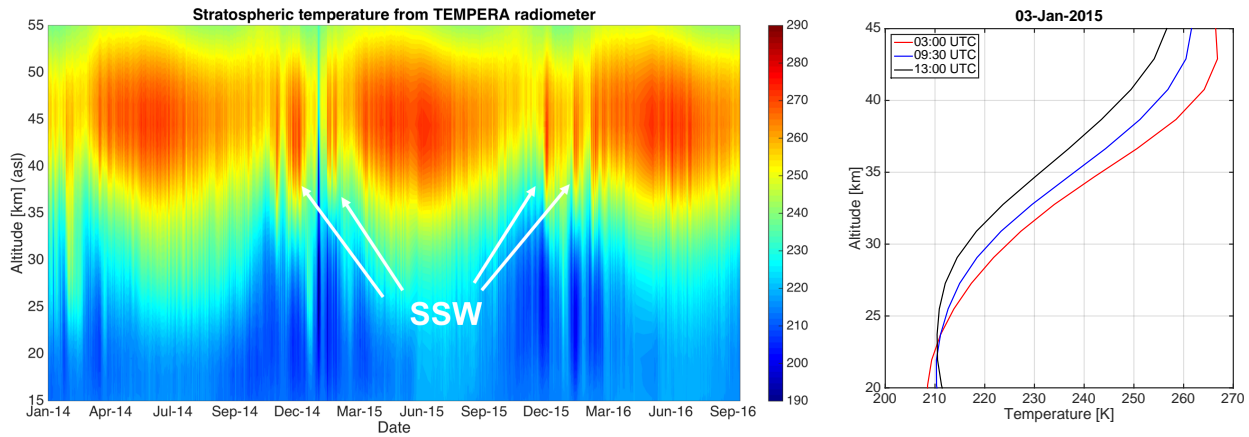


**Figure 5.** Left: Stratospheric temperature evolution from TEMPERA radiometer. Some SSW events ~~have been marked with~~ are indicated by white arrows.

higher temperatures in spring and summer than in autumn and winter. Some interesting episodes can also be observed during the three presented winters, in which strong increases of temperature are measured for short periods in the upper stratosphere and could be identified as SSW. ~~These increases of~~ These increases in temperature in the upper stratosphere ~~come many times~~ are often associated with a decrease ~~of in~~ temperature in the lower stratosphere ~~being this-~~, which is a pattern characteristic of SSW events. ~~The measurements presented in the plot~~ Figure 5 (right) shows an example of strong variation of temperature in the stratosphere for a winter day (3 January 2015). In this case, the temperature changed up to 15 K for some altitudes in the course of only 10 hours. These measurements show the importance of continuous observations for a fixed location, since the ~~variability of atmospheric parameters such as temperature evinces the necessity of measurements with good temporal resolution~~ important variations in temperature observed cannot be captured by only occasional measurements or measurements with poor temperature resolutions.

The temperature profiles from TEMPERA have been compared with ~~the ones those~~ from other instruments and ~~model, the~~ SD-WACCM model, all of which have different spatial and temporal resolutions. Figure 6 presents three representative examples of stratospheric temperature profiles ~~during winter, summer and~~: one in winter, one in summer and one in autumn. Measurements from the different instruments and model (re) ~~analyses show in general a~~ analysis show a generally good agreement in the range where they are comparable. Some ~~evident differences are observed~~ differences are evident in the upper stratosphere between MLS measurements and the other profiles on 4 February 2014. For the other two days ~~is~~ the lidar (black line) ~~the one that presents deviations is the source that exhibits deviations with~~ respect to the microwave measurements and the model in some ranges in the upper stratosphere. ~~We would like to~~ We point out the good agreement observed between TEMPERA radiometer and most of the other techniques in these three cases. The examples also illustrate the different vertical ranges and the spatial resolutions ~~from for~~ the different measurements. We can observe that radiosondes only cover the lower



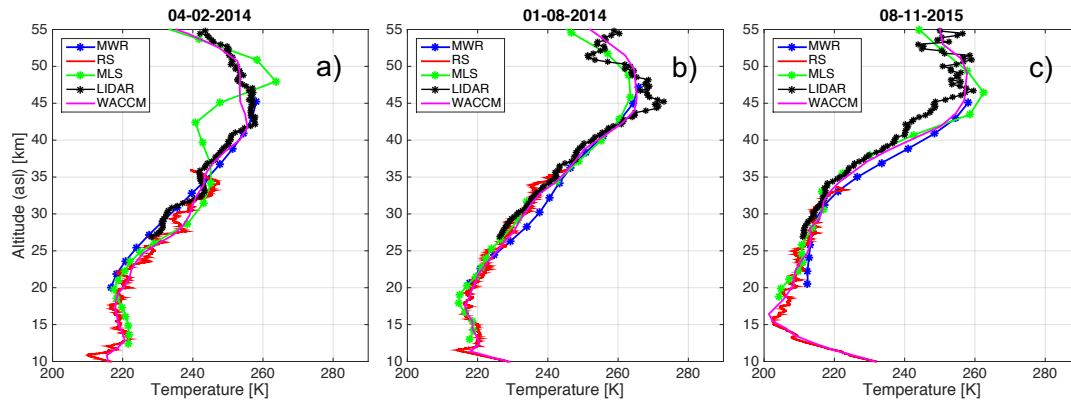


**Figure 6.** Stratospheric temperature profiles for night-time measurements from TEMPERA, RS, MLS, Lidar and WACCM model on (a) 4 February 2014, (b) 1 August 2014 and (c) 8 November 2015.

stratosphere but with a high spatial resolution, while lidar measurements provide information in the upper stratosphere. MLS and TEMPERA are able to cover almost the whole stratosphere although their spatial resolution is lower.

In order to validate the accuracy and errors of the temperature profiles from the TEMPERA radiometer a statistical analysis is performed with almost the three years of measurements (January 2014 – September 2016). For this period, TEMPERA profiles are compared with the ones from very different techniques as they are RS. In sections 4.1, 4.2, MLS satellite and lidar. In addition, profiles generated by 4.3 and 4.4 a comparison is made to, respectively, RS measurements, MLS measurements, lidar measurements and the SD-WACCM model have been validated with the ones from TEMPERA. In the next sections the different comparisons are presented. A multiway comparison between all of these is then presented in section 4.5.

#### 4.1 Comparison with RS

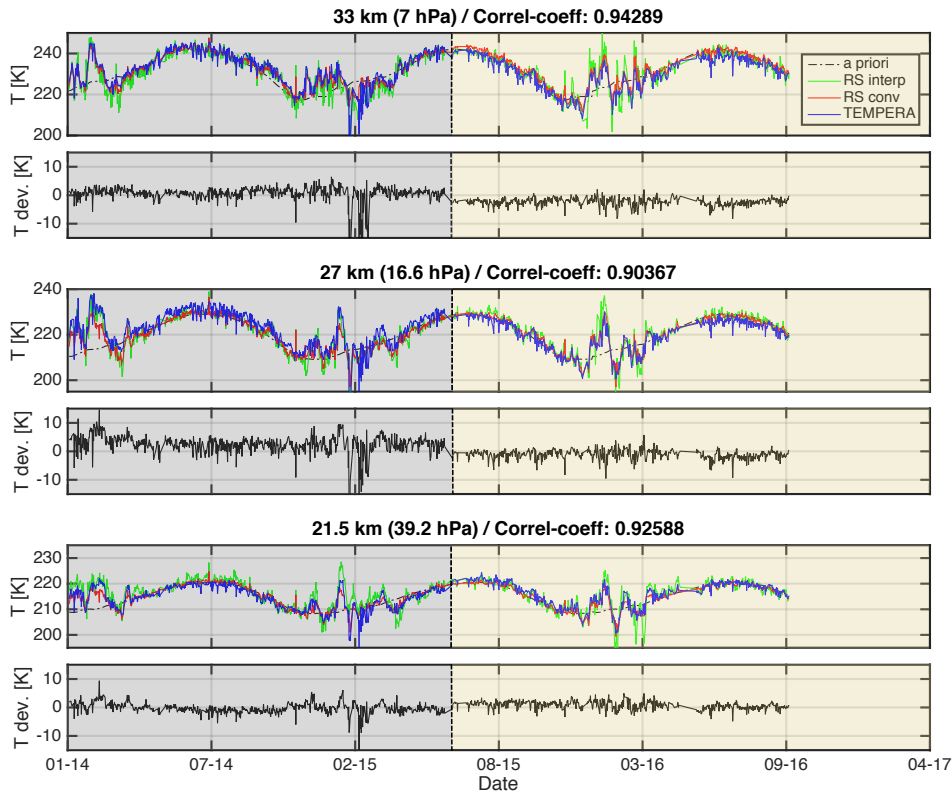
Stratospheric temperature profiles from TEMPERA have been compared with the ones from RS measurements for the period from January 2014 to September 2016. As it was indicated in previous sections RS are launched regularly radiosondes have been launched twice a day (11 and 23 UTC) at the aerological station at Payerne since 1954. The TEMPERA profiles closest in time to the RS launch launches have been selected in order to do this comparison. A total of 1489 pairs of profiles are used in this statistics these statistics, which were measured under all weather conditions except for rainy cases. The RS profiles were interpolated to the same altitude grid of TEMPERA radiometer, and completed in the upper part (above 35 km, no RS meas.) with the measurement from TEMPERA in order to use the with the TEMPERA measurements, since RSs usually do not reach altitudes higher than 30-35 km. Afterwards, the profiles were convolved using the averaging kernels of TEMPERA in the convolution of the RS profiles.

Figure 7 shows the temporal evolution of the stratospheric temperature at different altitudes from TEMPERA and RS along almost these three years of measurements for the campaign period. The interpolated temperatures from RS have also been plotted (green lines) in order to visualise the smoothing effect on them when they are convolved with the averaging kernels

of TEMPERA. In addition, the a priori temperature used for the TEMPERA inversions ~~has also been displayed.~~ is shown. The temperature deviations along this period between TEMPERA and the convolved measurements from RS are shown in the lower panels (black lines). We can observe in general a very good agreement between both instruments for the displayed altitudes with correlation coefficients higher than 0.9. An annual pattern is observed in the stratospheric temperature with higher temperatures in ~~summertime than in wintertime~~ summer than in winter. Again in this plot we can observe that the variability of the temperature is higher during winter than in other seasons, and some interesting events with a strong increase ~~of the in~~ temperature have been detected (January 2014 and 2015, February 2016). The temperature deviations between TEMPERA and RS are in general small with most of the values below 3 K, although some short periods with larger discrepancies are also found (e.g. February 2015). We can also observe from these plots that the deviations at 27 km altitude are larger and noisier than for the other two altitudes. A remarkable feature observed in the temperature deviation lines at all the profiles is a small step in summer of 2015. This step is more evident in the two higher altitudes (27 km and 33 km) where the deviations changed from positive to negative. The effect is smaller at the lowest altitude (21.5 km) ~~and where~~ it looks to have an opposite behaviour, changing from negative or almost zero deviations to positive deviations after the step happens. This change of tendency could be due to the fact that ~~there was a repair of an attenuator of an attenuator in~~ the FFT spectrometer was repaired in summer 2015. It seems that after this repair the brightness temperature spectra measured by the FFT were slightly affected and some small differences in the retrieved ~~temperature~~ temperatures are observed.

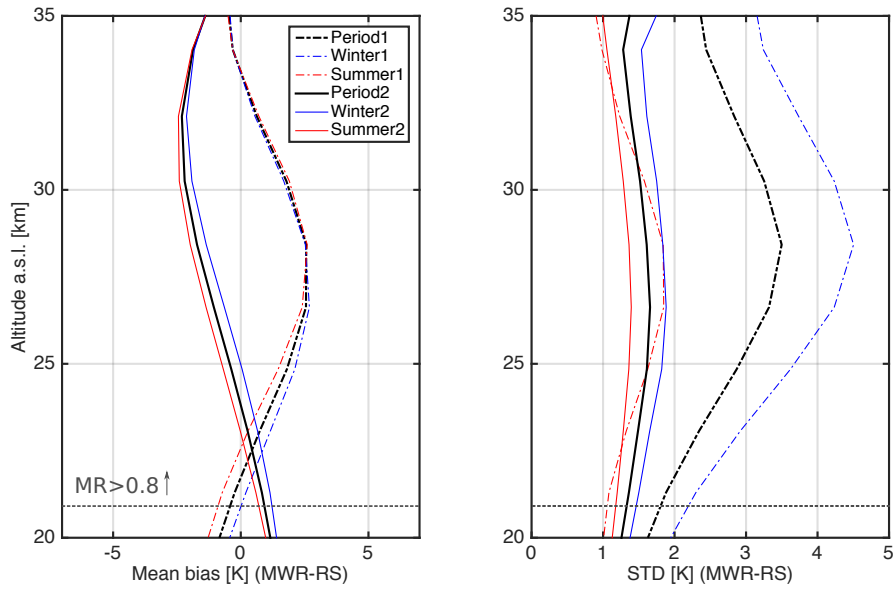
In order to take into account this instrumental modification and characterize possible changes in the accuracy and precision of the TEMPERA radiometer the statistical analysis between TEMPERA and the other measurements (RS, MLS, lidar and WACCM) is carried out over two different measurement periods. From here on, period 1 will ~~be referred as~~ refer to the period before the attenuator in the FFT spectrometer was changed (January 2014-June 2015) ~~while and~~ period 2 will ~~be referred as~~ refer to the period after this repair (July 2015-September 2016). In addition, ~~a seasonal distinction has been performed to take into account the larger atmospheric variability that could be observed during wintertime. The atmospheric conditions during wintertime could~~ the measurements have been split by season into winter and summer, with summer referring to April-September and winter October-March, inclusive. It is useful to make this distinction because there is a greater level of atmospheric variability in winter, which could produce larger deviations between the different measurements than ~~due to the different~~ those due to fundamental differences in the measurement techniques. ~~With this goal, the year has been split in two seasons, winter and summer. Winter measurements refer to those measurements taken between October and March while summer measurements refer to observations between April and September.~~

Figure 8 shows the mean and the standard deviations between TEMPERA and RS which have been calculated for all the measurements in each period (black lines) and also for winter and summer seasons of the different periods (blue and red lines, respectively). From this plot we can observe that there is a clear change in the mean bias between TEMPERA and RS for periods 1 and 2. The mean bias for period 1 ranged between -0.3 K at 20 km and 2.6 K at 28.5 km showing in general a positive deviation at most of the altitudes. The mean bias in period 2 showed negative values for most of the altitudes with values ranging between 0.9 K (20 km) and -2.3 K (32 km). There is also a clear difference in the standard deviation observed for both periods. Period 1 showed much larger standard deviations than period 2 with values that range between 1.9 K (21 km)



**Figure 7.** Stratospheric temperature evolution and temperature deviations at different altitudes for RS and TEMPERA. Different background colors are used to distinguish between period 1 and 2 (gray and light brown, respectively).

and 3.5 K (28.5 km). The standard deviations for period 2 were smaller and much more constant in height with values ranging between 1.3 K (34 km) and 1.7 K (26.5 km). These results show a change in the sign of the bias between TEMPERA and RS when the attenuator of the FFT spectrometer was repaired in June of 2015, although in term of absolute values the differences were not very significant. However, ~~concerning~~ the standard deviations ~~for~~ ~~period 2~~ ~~showed lower values than were smaller than for~~ period 1 indicating a higher precision of ~~the~~ TEMPERA radiometer after the repair ~~with~~ respect to the reference RS measurements. If we have a look at the seasonal behaviour of the bias for both periods we can observe that there are small differences between winter and summer. In the case of period 1 the maximum difference between winter and summer is 0.9 K and it is observed in the lower part, while for period 2 the differences are lower than 0.7 K. Much larger differences are found for the standard deviation between the two seasons for period 1 (dashed lines). While the standard deviations ranges between 0.9 K and 1.8 K in summer, the values ranged between 2 K and 4.5 K in winter, reaching the maximum standard deviation at 28.5 km. Although during period 2 the standard deviations in winter were also larger than in summer, the differences were not so remarkable (smaller than 0.5 K). These results show that there was a larger variability in the temperature deviations between



**Figure 8.** Mean temperature biases and standard deviations between TEMPERA and RS. A total of 1489 profiles have been compared (Period 1: 809 prof., dashed lines; Period 2: 680 prof., solid lines). The mean biases and the standard deviations for each periods are represented by black lines. The winter season is indicated with blue lines while the summer is indicated by red lines (Winter1: 421 prof.; Summer1: 388 prof.; Winter2: 289 prof. Summer2: 391).

TEMPERA and RS during the winters of period 1. It is something that could be expected from the temperature evolution showed in Fig. 7 that showed larger discrepancies specially during winter 2015.

## 4.2 Comparison with Aura/MLS

5 The stratospheric temperature profiles from TEMPERA have also been compared with ~~the ones those~~ obtained from the MLS instrument on board ~~of the~~ Aura satellite. As ~~it was~~ indicated in section 2 the temperature profiles used for MLS correspond to the version 4 retrievals. In order to select the temperature profiles from MLS to be used in the comparison we chose those ~~ones~~ that were collocated with the measurement site, ~~and for our criterion it was~~ which by our criteria meant that the MLS measurements ~~inside of the range of~~ were within  $\pm 1^\circ$  ( $\pm 110$  km) of the measuring site in latitude and  $\pm 5^\circ$  ( $\pm 460$  km) in

10 longitude. The data were also restricted to cases with near time-coincident between TEMPERA and MLS, which means that the MLS profiles were taken during the period of the spectral integration for the TEMPERA measurements. A total of 367 profiles were obtained under these criteria and for all weather conditions excluding rainy cases. The ~~temperature profiles of~~ MLS-MLS temperature profiles were interpolated to the pressure grid of TEMPERA and these profiles were convolved using the averaging kernels of TEMPERA as ~~it was~~ described in section 3.

15 Figure 9 shows the evolution of the stratospheric temperatures and the deviations between TEMPERA and MLS at 3 different altitude levels. Similar patterns to ~~the ones those~~ observed in Fig. 7 are found in this plot (although with less data), observing an

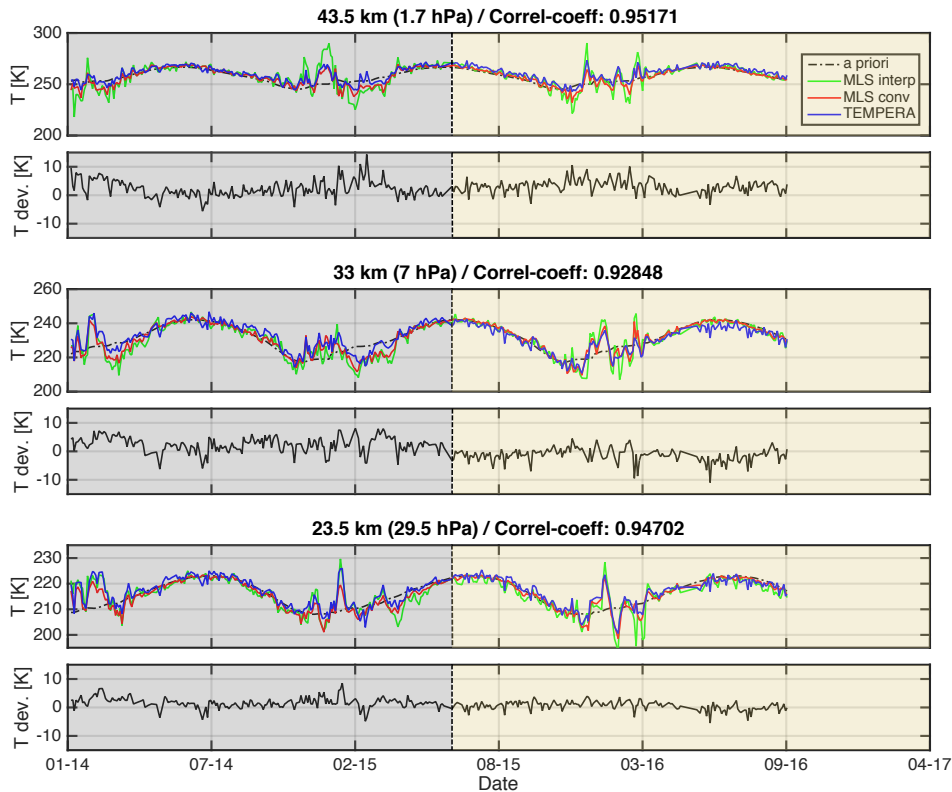


**Figure 9.** Stratospheric temperature evolution and temperature deviations at different altitudes for TEMPERA and MLS. Different background colors are used to distinguish between period 1 and 2 (gray and light brown, respectively).

annual cycle with higher temperature temperatures in summer than in winter and with a larger variability during wintertime. We can observe from these plots a very good agreement between both instruments despite the very different type of observations that we are comparing (ground-based against satellite measurements). This good agreement is also observed when strong variations of temperature are exhibited in temperature occur in a short interval time as it time interval, as can be seen in the winter of 2016 and it, and is confirmed by the high correlation coefficient (larger than 0.92) found at the different altitudes. The temperature deviations (TEMPERA-MLS) observed are in general small, although we can observe some larger discrepancies for some measurements (reaching deviations of 10 K) mainly during wintertime. Differences between TEMPERA and MLS retrievals can arise from several factors, including differences due to spatio-temporal inhomogeneities due to arising from synoptic variability which can be more important during winter, differences in vertical resolution or interpolation techniques, interpolation techniques, or measurements errors of from both instruments.

The mean and the standard deviations between of the difference between the TEMPERA and MLS for all the measurements of the two measurements for both periods described in the previous section and also for the different seasons have been plotted

in Figure 10. From this comparison, a clear change in the mean bias is again observed between both periods in the lower part of the stratosphere (from 20 to 37 km). In that range, the mean bias in ~~the~~ period 1 was  $2.5 \pm 1.3$  K, reaching a maximum deviation of 4.1 K at 28.5 km, while for period 2 the mean bias was  $-0.4 \pm 0.9$  K with a maximum negative deviation of  $-1.4$  K at 30 km. In the upper part (between 38 and 50 km) the differences in the biases were not so significant with a mean value of  $1.7 \pm 0.5$  K for period 1 and  $2.3 \pm 0.7$  K for period 2. The standard ~~deviation shows again~~ deviations again show higher values for period 1 than for period 2, although the differences were smaller than in the comparison with RS. The mean standard deviations in the range between 20 and 50 km were  $2.4 \pm 0.6$  K for period 1 and  $2.0 \pm 0.4$  K for period ~~2-2~~.

This comparison also shows a seasonal behaviour for the mean and the standard deviation of the temperature differences between TEMPERA and MLS for both periods. For period 1 there was a positive bias for both seasons ~~almost in in almost~~ the whole column with larger values in winter than in summer. The mean bias in the lower part (20-35 km) was  $3.3 \pm 1.2$  K in winter and  $1.9 \pm 1.4$  K in summer. The discrepancies were even larger in the upper part (35-50 km) showing a much lower bias in summer ( $0.4 \pm 0.4$  K) than in winter ( $2.8 \pm 0.7$  K). During period 2 the differences between the biases in winter and summer were quite constant in altitude and they were always lower than 1.6 K. The standard deviations of the temperature differences showed higher values in winter than in summer for both periods. For period 1 the mean standard deviation for the whole range (20-50 km) was  $2.5 \pm 0.5$  K in winter reaching a maximum value (3.1 K) at 28.5 km while for period 2 the mean standard deviation was  $2.1 \pm 0.5$  K with a maximum value of 2.6 K at 32 km. The standard deviations in summer for both periods were very similar with mean values for the whole altitude range (20-50 km) of  $1.8 \pm 0.6$  K in period 1 and  $1.7 \pm 0.5$  K in period 2. These results ~~show again~~ again show the lower temperature discrepancies observed between TEMPERA and the MLS satellite during summertime. The biases found in this comparison are similar to ~~the ones~~ those reported by Schwartz et al. (2008) for a comparison between MLS version 2.2 retrievals and different analyses and observations (GEOS-5, ECMWF, radiosondes, AIRS/AMSU, etc), where the biases ranged between -2.5 K and ~~+1-~~ 1 K.

The MLS measurements have also been compared with the ones from RS in the range where they were comparable (lower stratosphere). Only collocated MLS profiles (~~with the same criteria explained~~ according to the criteria as used above) and measured ~~in an temporal interval lower than~~ within 4 hours ~~to of~~ the RS launch were selected for the comparison. A total of 323 ~~pair~~ pairs of profiles fulfilled these criteria and were used for ~~this~~ these statistics. The RS profiles were interpolated to the pressure grid of MLS in order to perform the direct comparison of their profiles. Figure 11 shows the mean and the standard deviation for this comparison. We can observe that the mean bias ranges ~~between from~~ -1.7 K at 19 km ~~and to~~ +1.4 at ~~19.6-15~~ km. The standard deviation of the temperature differences between MLS and RS was quite constant ~~in altitude~~ with altitude, with a mean value of  $1.7 \pm 0.2$  K and a maximum ~~standard deviation value~~ of 2.2 K reached at 31 km. We ~~can~~ note that the bias and the standard deviation observed between MLS and RS ~~is are~~ very similar to the values observed in the comparison between TEMPERA and RS in period 2 (biases ranging between -2.3 K and 0.9 K and the standard deviations between 1.3 K and 1.7 K). The slight underestimation of the temperature in most of the altitudes found for MLS versus RS in this study agrees with the results obtained by Schwartz et al. (2008) between MLS and different sources.

### 4.3 Comparison with lidar measurements

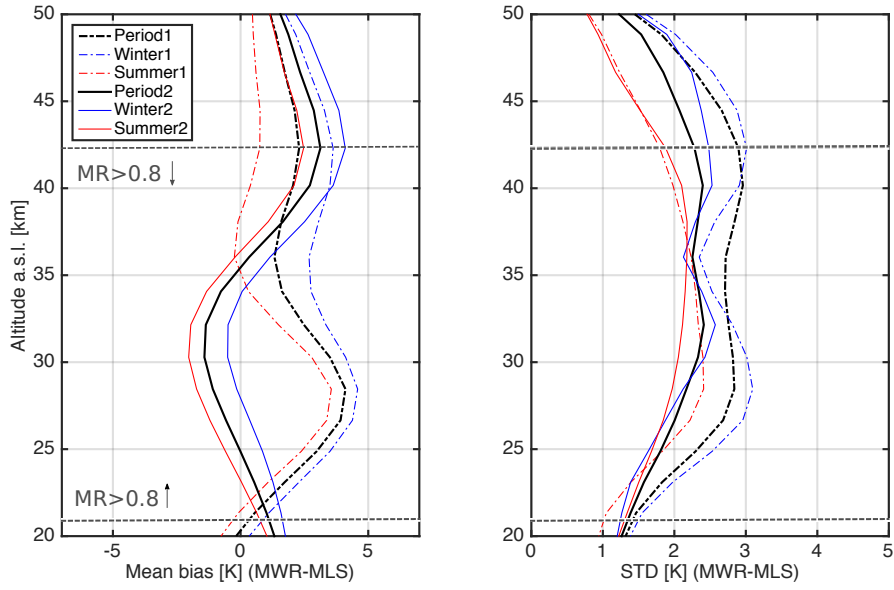


**Figure 10.** Mean temperature [biases](#) and standard deviations between TEMPERA and MLS. A total of 358 profiles have been compared (Period 1: 192 prof., dash lines; Period 2: 166 prof., solid lines). The mean and the standard deviations for each period are represented by black lines. The winter season is indicated with blue lines while the summer is indicated by red lines (Winter1: 103 prof.; Summer1: 89 prof.; Winter2: 67 prof. Summer2: 99).

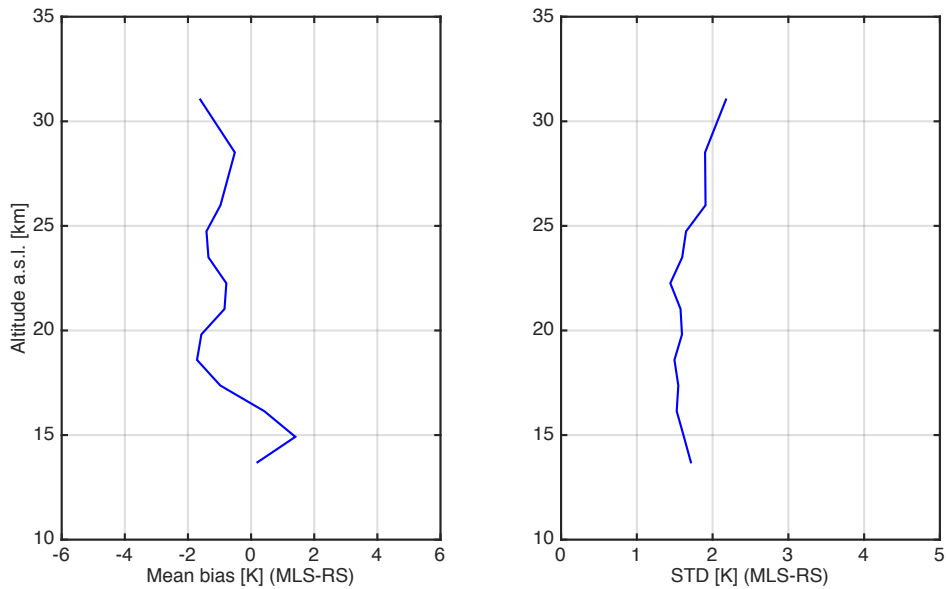


**Figure 11.** Mean [bias](#) and standard temperature deviation between MLS and RS.

The TEMPERA radiometer has also been compared with an active remote sensing instrument, a Rayleigh lidar. This lidar is operated at Hohenpeißenberg station (Germany) which is located around 400 km Northwestward-northwest of Payerne. Despite the distance between both instruments, we wanted to evaluate the agreement in the stratospheric temperature between these very different techniques. A total of 192 profiles have been compared for all weather conditions (excepting-except for rainy cases) for the period from January 2014 to July 2016. As in the previous comparisons the lidar profiles were also-interpolated to the pressure grid of TEMPERA radiometer and then these profiles were convolved using the averaging kernel of TEMPERA. Since the Rayleigh lidar only provides temperature information above approximately 28 km (below this the measurements would be affected by stratospheric aerosol), the gap below this altitude was filled with coincident measurements from TEMPERA in order not-to-modify-to avoid modifying the averaging kernel used by TEMPERA for the convolution.

Figure 12 shows the stratospheric temperature evolution from TEMPERA and the lidar at three different altitude levels. For the lowest altitudes shown here (29.5 km, asl), the temperature from RS has also been plotted since at this altitude there were measurements from the three instruments. We can observe from this figure that there is a-good agreement between TEMPERA and the lidar in the upper stratosphere, with correlation coefficients larger than 0.94 for the two highest altitudes. This coefficient is lower (0.9) for the lowest altitude (29.5 km, asl). The agreement between the lidar and the RS in this lowest altitude is better than for TEMPERA with a correlation coefficient of 0.96. The evolution of the temperature deviations between TEMPERA and lidar at the three altitudes shows small discrepancies for both techniques along-the-year-over the measurement period, with the values in most measurements below 5 K. The biggest differences were found at the lowest altitude (29.5 km, asl), where a clear change of bias was observed after summer 2015.

Figure 13 shows the mean bias and the standard deviation for all the measurements in periods 1 and 2 in addition to seasonal profiles. Mean bias profiles show again a clear change in the tendency of the biases of both periods, being more evident in the lower stratosphere (below 35 km). In this lowest altitude range the mean biases were  $2.7 \pm 1.3$  K for period 1 and  $-1.2 \pm 0.4$  K for period 2. Above 35 km the differences between the biases were smaller with a largest-larger bias for period 2 ( $2.3 \pm 0.9$  K versus  $1.3 \pm 0.4$  K in period 1). Similar behaviour to the other comparisons has been observed for the standard deviation with largest-larger values during period 1 than during period 2. The mean values for the whole altitude range were  $2.9 \pm 0.3$  K for period 1 and  $2.5 \pm 0.2$  K for period 2. A-seasonal-Seasonal behaviour is observed in the bias and standard deviation for both periods. The seasonal biases showed a vertical oscillation with different tendencies for both periods in the lower and upper part of the stratosphere. For the lower part (28-35 km) the mean biases for period 1 (period 2) were  $3.2 \pm 1.1$  K ( $-0.7 \pm 0.4$  K) in winter and  $1.9 \pm 1.5$  K ( $-2.1 \pm 0.3$  K) in summer. In the upper part (35-50 km), a general positive bias was observed between TEMPERA and the lidar where the mean biases for period 1 (period 2) were  $2.2 \pm 0.6$  K ( $2.9 \pm 1.1$  K) in winter and  $-0.3 \pm 0.3$  K ( $1.1 \pm 0.9$  K) in summer. The standard deviations showed larger values in winter for both periods than in summer. The highest standard deviations were again observed in the winter of period 1. The mean standard deviations in the whole column were-for period 1 (period 2) were  $3.1 \pm 0.4$  K ( $2.6 \pm 0.3$  K) in winter and  $2.0 \pm 0.3$  K ( $1.7 \pm 0.4$  K) in summer.





**Figure 12.** Stratospheric temperature evolution from TEMPERA, lidar and RS. Different background colors are used to distinguish between period 1 and 2 (gray and light brown, respectively).

#### 4.4 Comparison with SD-WACCM

10 A first validation of the stratospheric temperature from SD-WACCM (Whole Atmosphere Community Climate Model with  
 Specified Dynamics) has also been carried out in this study. SD-WACCM is the whole atmosphere component of CESM  
 (Community Earth System Model) (Kunz et al., 2011; Lamarque et al., 2012). CESM is a coupled climate model which means  
 that it consists of separate models for different parts of the climate system which interact via the coupler module. There are  
 models for ocean, atmosphere, land, sea ice, land ice and rivers. CESM allows to combine the above models to a component  
 15 set for the simulation.

The Specified Dynamics (SD) used in these simulations means that the model is nudged by meteorological analysis fields  
 by 10% at every internal time-step up to an altitude of 50 km. This means 90% of the model and 10% of the nudging data are  
 taken. The fields that are nudged are temperature, horizontal winds, surface wind stress, surface pressure and heat fluxes from

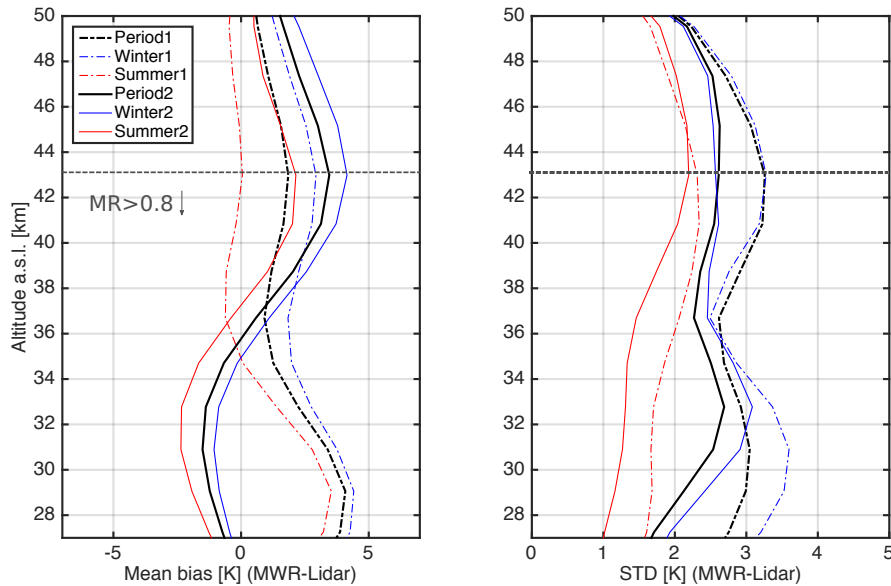


**Figure 13.** Mean temperature deviation between TEMPERA and lidar. A total of 192 profiles have been compared (Period 1: 117 prof., dash lines; Period 2: 75 prof., solid lines). The mean [bias](#) and the standard deviations for each period are represented by black lines. The winter season is indicated with blue lines while the summer is indicated by red lines (Winter1: 73 prof.; Summer1: 44 prof.; Winter2: 49 prof. Summer2: 26).

the surface. The nudging data [is are](#) from the Goddard Earth Observing System version 5.0.1 (GEOS-5) Data Assimilation and  
 20 is provided every 6 hours, in between the data are interpolated.

The altitude range for SD-WACCM is from ground to 140 km (asl). The altitude resolution ranges from 0.5 to 4 km (with lower resolution at higher levels) and with a total of 88 layers in the whole atmosphere. The grid resolution is 1.9° latitude by 2.5° longitude.

The stratospheric temperatures from SD-WACCM have been compared with the almost continuous stratospheric temperature  
 25 profiles measured by [the](#) TEMPERA radiometer for the period from January 2014 to April 2016. A total of 6868 profiles were selected [for comparison](#) under all weather conditions except rainy conditions. Figure 14 shows the stratospheric temperature evolution along this period for TEMPERA and WACCM. [A good Good](#) agreement is observed in general between both temperature sets. We can observe [as that](#) the temperature from the model follows the same pattern as [for](#) TEMPERA, with the same annual cycle and detecting the same structures in time and also in altitude. [It is worth to point out Note](#) the good agreement  
 30 observed during winters, where strong increases [of in](#) temperatures are produced for short periods and can be observed in both data sets. The differences between TEMPERA and WACCM are more evident above 50 km (asl), but above this altitude the measurement response for TEMPERA is low (lower than 0.6) since the weight of the measurements is small and [so it](#) should not be considered in the comparison.

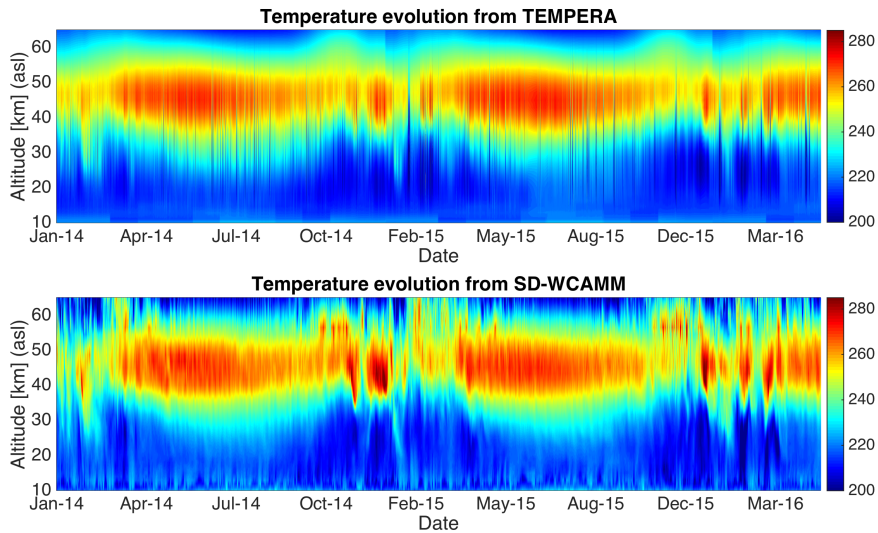


**Figure 14.** Stratospheric temperature from TEMPERA radiometer (upper panel) and WACCM model (lower panel).

The temperature profiles from SD-WACCM have been interpolated and convolved as ~~it was explained~~ described in section 3 ~~in order to compare with the ones to allow comparison with those~~ from TEMPERA. Figure 15 shows the evolution of the temperature at three altitude levels and the differences between both (TEMPERA-WACCM). The good agreement observed from these plots is ~~proven~~ particularly shown by the low temperature deviation values ~~along the time~~ (lower than 5 K ~~in most of the time~~) and the large correlation coefficient (larger than 0.92). Despite this good agreement, we also find some periods with larger discrepancies between the measurements and the model, ~~specially~~ especially during winter time ~~and being more evident~~ , most markedly in winter 2015. ~~It is worth to point out the very robust statistics that we are showing~~ Note that the statistics shown in this section, ~~with are particularly robust, since~~ almost 7000 pairs of temperature profiles are compared.

We have also calculated the bias and the standard deviation for this comparison between the TEMPERA radiometer and the WACCM model (Fig. 16). It is again very obvious from ~~this statistics~~ these statistics that there is a strong change in the biases between periods 1 and 2, with a very different tendency in the lower stratosphere than in the upper. The mean biases for the lower part (20-35 km) were  $1.4 \pm 1.1$  K for period 1 and  $-1.0 \pm 1.3$  K for period 2. ~~While 2, whilst~~ the mean biases for the upper stratosphere (35-50 km) were  $1.0 \pm 0.7$  K for period 1 and  $1.7 \pm 1.1$  K for period 2. ~~It is worth to remark the almost negligible~~ The seasonal behaviour observed in the biases was almost negligible for both periods.

From the standard deviation figure (Fig. 16, right) we can observe that much larger values are obtained for period 1, with a mean value in the whole column of  $2.9 \pm 0.6$  K and a maximum standard deviation of 3.8 K at 29 km. ~~This~~ These large standard deviations observed during period 1 ~~is are~~ strongly influenced by the large values observed during winter time (blue dashed line) ~~that reached a maximum~~ , when a maximum mean standard deviation of 4.7 K at 29 km was reached. The rest of the standard deviation profiles show very similar values between them, increasing slightly in the lower part (up to 30 km), and

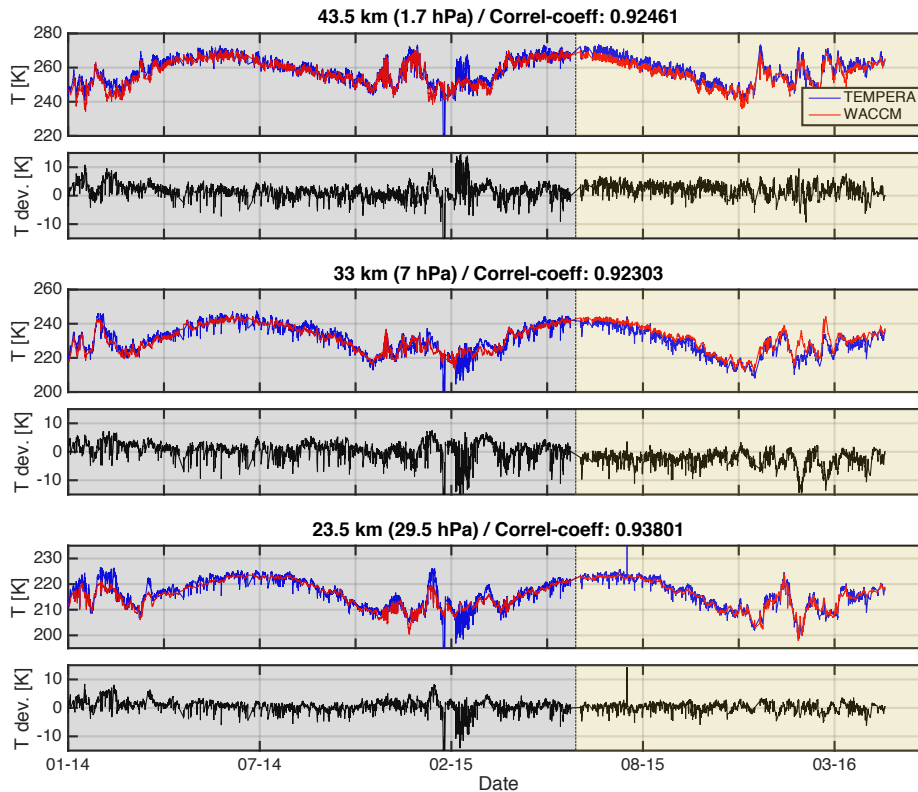


**Figure 15.** Stratospheric temperature evolution from TEMPERA and WACCM. Different background colors are used to distinguish between period 1 and 2 (gray and light brown, respectively).

keeping close to constant values above this altitude. The smallest values are found in summer with a mean bias in the whole column of  $1.8 \pm 0.4$  K for period 1 and  $1.5 \pm 0.3$  K for period 2.

#### 4.5 All measurements and model versus TEMPERA

In order to summarize the intercomparison carried out between TEMPERA and the different measurement techniques and model we have plotted ~~together~~ the biases and the standard deviations for all the comparisons together (Fig. 17). Since we are interested in evaluating the accuracy and precision of TEMPERA radiometer against other measurements in this study we have only displayed in Fig. 17 the biases and the standard deviations obtained for the summer season ~~which~~, since it is less affected by atmospheric variability than ~~wintertime~~ the winter measurements.

The mean bias plot (Fig. 17, left) shows a clear change of biases between TEMPERA and all the other measurements ~~for~~ between the first (dashed lines) and the second (solid lines) period (before and after the repair of the FFT spectrometer's attenuator). We can observe that there is a persistent vertical oscillation for all the profiles in both periods causing a different behaviour of the biases in the lower and upper stratosphere. This oscillation has an amplitude of around 2 K and a periodicity of

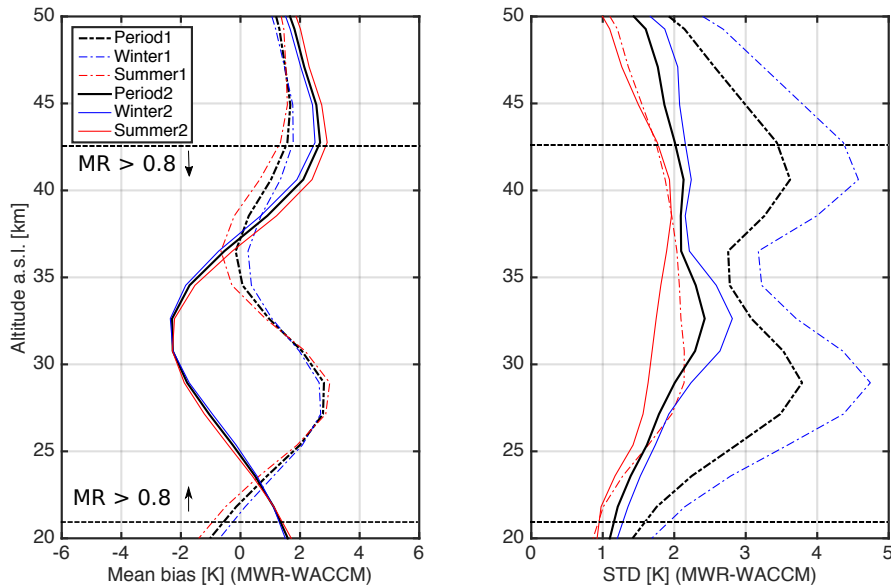


**Figure 16.** Mean temperature deviation between TEMPERA and the WACCM model. A total of 6868 profiles have been compared (Period 1: 4339 prof., dash lines; Period 2: 2529 prof., solid lines). The mean and the standard deviations for each period are represented by black lines. The winter season is indicated with by blue lines while the summer is indicated by red lines (Winter1: 2361 prof.; Summer1: 1978 prof.; Winter2: 1473 prof. Summer2: 1056).

roughly 20 km. Similar behaviour was observed for the MLS measurements when they were compared with different sources (Schwartz et al., 2008). The change of tendency in the bias between both periods is more evident in the lower stratosphere (below 35 km) where we can observe that almost for for almost all the altitude levels the biases changed change from positive to negative values in all the comparisons. Another remarkable point is the consistency between the different biases in each period, showing small differences between them (below 1K) for most of the altitudes, specially especially for period 2. For period 1, the maximum deviations were deviation was found at 28.5 km, with a maximum value of 3.6 K for the comparison with the MLS satellite. Below this altitude, an almost identical bias between the comparison with RS and WACCM model is found. In the upper stratosphere the biases were between -0.6 K and 1.5 K showing the lowest bias with the lidar, and the smallest bias was found in the lidar comparison. For period 2 the values of the different biases ranged between -2.4 K (at 32 km) and a maximum positive bias of 2.9 K (at 43 km) was found for, the latter being found with the comparison with WACCM.

As we already mention the differences between the different comparisons for period 2 were smaller than for period 1 showing the consistency between the RS, MLS, lidar measurements and also WACCM simulations.

Fig. 17(right) shows the standard deviations of the differences between TEMPERA and the different measurements and model. In general we can observe that there was a reduction in the standard deviations for all the comparisons in period 2, indicating that the precision of TEMPERA improved after the attenuator was repaired. Next, we will focus our discussion on period 2, when we consider that TEMPERA was operated in its optimal status operating optimally. For this period, we can

observe that standard deviations were always lower than 2.2 K ~~and this maximum values was~~, with this maximum value being reached at 45 km ~~for in~~ the comparison with the lidar. The lowest standard deviation in the lower stratosphere (< 35 km) was found for the comparison with RS ~~and~~, with the mean value ~~of the standard deviation~~ in this range ~~was being~~  $1.3 \pm 0.1$  K. The highest standard deviations in the lower stratosphere ~~was found for~~ were found in the comparison with MLS ( $1.3 \pm 0.1$  K). These results evidence a better precision ~~of from the~~ TEMPERA radiometer when it is compared with the in situ reference  
5 technique of RS in the lower stratosphere. This result makes sense since RS is the technique with the lowest errors (0.2 K for temperature) and the comparison between TEMPERA and RS is the one that should present lower atmospheric variability between both measurements since the RS are launched ~~in from~~ the same location ~~that where~~ TEMPERA is operated.

In the middle stratosphere (between 30 and 40 km) the lowest standard deviations were found for the comparison with lidar with a mean value of  $1.4 \pm 0.2$  K. However, above this altitude (40 km) the standard deviation with respect to lidar is the  
10 ~~deviations with lidar are the~~ largest (~~1.42, 2 ± 0.2 0.3~~ K). In this upper part the lowest standard deviations were found for the comparison with MLS and WACCM. A common pattern that is observed in all the comparisons is that the standard deviations decrease slightly with altitude in the last kilometres of the stratosphere. This behaviour is due to a greater weight of the a priori temperature profile used in the TEMPERA retrievals and also in the convolved profiles in these altitudes since the measurement response presents lower values for high altitudes (around 0.6 at 48 km).

15 Table 1 presents the different biases and standard deviations obtained in the lower and upper stratosphere for all the comparisons during summertime in period 2. These values ~~could be considered as are~~ the most representative way of characterizing the accuracy and precision of ~~TEMPERA radiometer. Since the~~ TEMPERA radiometer since they correspond to the period when TEMPERA was running with the repaired attenuator (period 2) and also when the measurements were ~~less least~~ affected by atmospheric variability (summertime).

20 We ~~would like to~~ end by highlighting the consistency found between the standard deviations of the different comparisons and the observation errors of the TEMPERA retrievals. As ~~we already~~ mentioned in section 3.1 the OEM also estimates the observation, smoothing and total errors of the TEMPERA inversions (Fig. 4e). The standard deviations found in the different comparisons are ~~somehow partly~~ related to the observation error of TEMPERA but also to the errors associated with the other measurements and the atmospheric mismatches. If we assume that the random errors in TEMPERA (D1), in the other instruments (D2) and in the atmospheric mismatching (D3) are independent, then the observed standard deviation (DT) should  
5 be given by  $DT^2 = DT1^2 + DT2^2 + DT3^2$ . For example, if we consider the observation error of TEMPERA provided by OEM (0.8 K), the errors for the lidar (0.7 K) and the mean observed standard deviation for the comparison between TEMPERA and the lidar (1.1 K) we would conclude that the errors associated with atmospheric mismatches should be 0.3 K, which is a realistic value and ~~in this way~~ shows the consistency between the observed standard deviations and the observation errors of the different measurements.

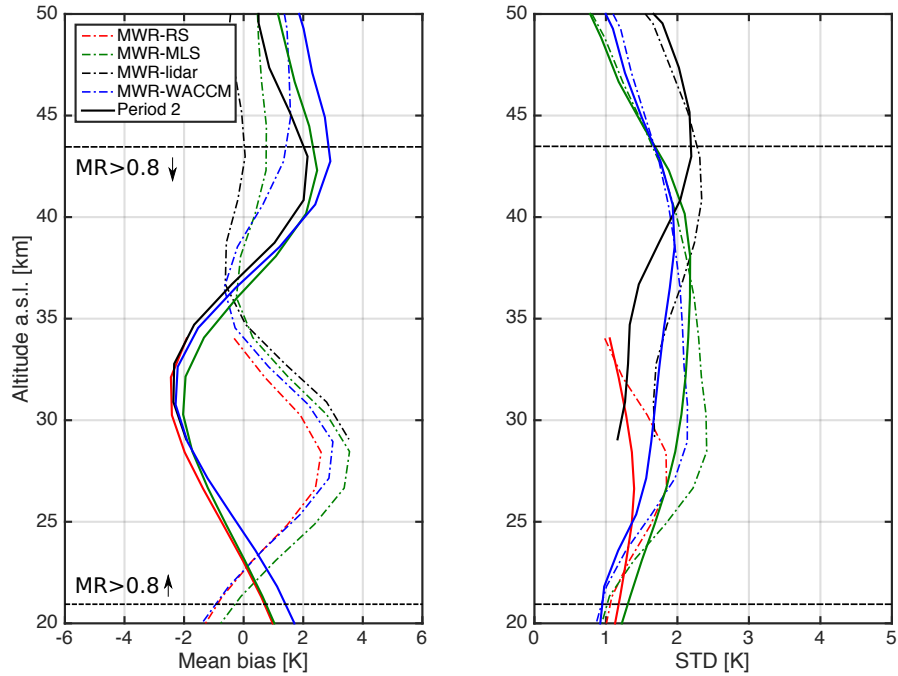


**Figure 17.** Mean and standard temperature deviations between the TEMPERA radiometer and the measurements from the different instruments and WACCM.

**Table 1.** Range of bias-biases and standard deviations between of the TEMPERA radiometer when compared with RS, MLS, lidar and WACCM with TEMPERA radiometer measurements/model results.

		MWR-RS	MWR-MLS	MWR-lidar	MWR-WACCM
lower strat. (20-35 km)	BIAS	-1.3±1.1	-1.0±1.0	-1.1±1.3	-1.0±1.3
	STD	1.3±0.1	1.8±0.3	1.1±0.2	1.5±0.3
upper strato. (35-50 km)	BIAS		1.5±0.9	1.1±0.9	1.9±1.1
	STD		1.7±0.5	1.9±0.3	1.6±0.3

## 10 5 Conclusions

Almost-Nearly three years of measurements of stratospheric temperature profiles from a relatively new ground-based microwave radiometer (TEMPERA) have been intercompared with the-ones-those from different measurement techniques as they are: RS, MLS satellite and Rayleigh lidar and also from the SD-WACCM model. TEMPERA measurements were carried out at the aerological station of MeteoSwiss at-in Payerne from January 2014 to September 2016. Ground-based microwave measurements present-as-main-offer the advantages that they can provide unattended continuous measurements of temperature profiles in almost all weather conditions with a reasonable-reasonably good spatial and temporal resolution. The stratospheric

temperature profiles (from 20 to 50 km) were obtained from TEMPERA measurements using OEM by means of the radiative transfer model ARTS/QPack. All the profiles from the other techniques (RS, MLS and lidar) and from the WACCM model were interpolated to the TEMPERA pressure grid and then convolved using the averaging kernel of this radiometer in order to be compared with the ones profiles from TEMPERA.

The temperature evolutions measured at different altitudes of by TEMPERA and the different measurements and model other techniques, as well as the model, showed in general a very good agreement with a high correlation (always larger than 0.9) between the compared datasets. These datasets. The stratospheric temperature evolutions showed a larger variability during wintertime and also evidenced larger discrepancies between TEMPERA and the other datasets during that those periods. A small step in the temperature deviations was observed in July of 2015 for the different comparisons, and it was related with which was related to the repair of an attenuator in the FFT spectrometer of TEMPERA. This repair caused a small modification change in the measured brightness temperature from TEMPERA and therefore in the retrieved temperature profile from this radiometer. For this reason, and in order to take into account this instrumental the instrument modification and characterize possible changes in the accuracy and precision of TEMPERA radiometer, the statistical analysis was carried out over two different measurement periods (before and after the modification). In addition a seasonal distinction (winter and summer) was considered in the statistics to take into account the larger atmospheric variability that could can be observed during wintertime and which could produce larger deviations between the instruments due to the atmospheric conditions.

The accuracy and the precision of TEMPERA radiometer have the TEMPERA radiometer has been evaluated by means of the bias and the standard deviation between TEMPERA and other measurements and model outputs relative to other measurement techniques and model output (RS, MLS, lidar and WACCM), as well as the standard deviation of the difference between the measurements. The stratospheric temperature comparison between TEMPERA and the other datasets showed a clear change in the biases between periods 1 and 2 (before and after the repair of the attenuator) in all the statistics. For the lower stratosphere (20-35 km) the biases changed from positive values in period 1 to negative values in period 2. The smallest mean deviations were observed in the comparison with RS, with values always lower than  $\pm 2.5$  K. The largest biases were observed for the comparisons with MLS and the Rayleigh lidar reaching maximum deviations of around +4.5 K at some altitudes in period 2. In general the biases were smaller and with negative sign negative for all the comparisons during period 2, indicating a slight underestimation of the temperature by TEMPERA radiometer in that period.

In the upper part of the stratosphere (above 35 km) the differences between both periods were not so evident, and general generally positive biases were observed in both periods for all the comparisons. The deviations in this upper part were always lower less than 4.5 K. We would like to point out the that only weak seasonal behaviour was observed for the biases in the comparisons with RS and WACCM while, whereas it was more pronounced for the comparison with MLS and lidar, specially the lidar, especially in period 1.

The standard deviations obtained from the different statistics showed again very different results between both in the two periods. Larger values were observed for all the comparisons in period 1 than in period 2, indicating that the precision of TEMPERA radiometer improved after the repair of the spectrometer's attenuator. The standard deviations were especially high in wintertime of during period 1, reaching maximum values of around 4.5 K for the comparison with RS (at 28 km) and



MLS (28 km and 41 km). In period 2 the standard deviations during winter were also larger than in summer but with smaller differences (except for the lidar in the lower part of the stratosphere). These results confirmed the larger atmospheric variability that can be found during wintertime and which ~~produce~~ produces a lower agreement in the temperature measurements between  
5 the different instruments, especially when the horizontal distance between them is large.

Finally, the accuracy and the precision of the TEMPERA radiometer have been characterized by means of the bias ~~and the standard deviation of this radiometer versus the different measurements and model obtained~~ relative to the different measurement and model values, as well as by the standard deviations of temperature differences between TEMPERA and the other values. All of this was done during period 2 (instrument in optimal conditions) and in summer (less affected by  
10 atmospheric variability). ~~This~~ These statistics in the lower stratosphere (below 35 km) showed mean biases ranging between 1.0 and 1.3 K (max. for RS and min. for MLS) and mean standard deviations that ranged between 1.1 and 1.8 K (max. for MLS and min. for lidar). While in the upper stratosphere (above 35 km) the mean biases ranged between 1.1 and 1.9 K (max. for WACCM and min. for lidar) and the mean standard deviations ranged between 1.6 and 1.9 K (min. for WACCM and max. for lidar). The standard deviations observed in the different comparisons were consistent with the observation errors that are  
15 expected from the different instruments, indicating that it is a good measure of the ~~instrumental~~ instrument errors.

From all these intercomparisons we can conclude that ~~TEMPERA radiometer has shown a very good performance to determine the temperature~~ the TEMPERA radiometer performed well at determining temperatures in the stratosphere. Continuous TEMPERA measurements will ~~allow~~ in the future make it possible to carry out temperature trend ~~analysis~~ analyses, which are an important component of ~~the~~ global change. These trends can provide evidence of the roles of natural and anthropogenic climate change mechanisms. Stratospheric temperature changes are also crucial for understanding stratospheric ozone variability and trends, including predicting future changes. In addition, measurements with a high temporal resolution in a fixed location will ~~also allow~~ make it possible to characterize the local thermodynamics, which can be ~~especially~~ specially  
5 interesting during wintertime.

*Acknowledgements.* We thank MeteoSwiss and in particular Dominique Ruffieux, Ludovic Renaud, Philippe Overney and Jean-Marc Aellen for hosting our instrument and for the support on-site. We would also like to thank to Dr. Peter Speirs for his contribution with the language revision of this manuscript. This work has been funded by the Swiss National Science Foundation under grant 200020-160048 and MeteoSwiss in the framework of the GAW project "Fundamental GAW Parameters by Microwave Radiometry".

## 10 References

- Anderson, G. P., Clough, S., Kneizys, F., Chetwynd, J., and Shettle, E. P.: AFGL atmospheric constituent profiles (0.120 km), Tech. rep., DTIC Document, 1986.
- Aumann, H. H., Chahine, M. T., Gautier, C., Goldberg, M. D., Kalnay, E., McMillin, L. M., Revercomb, H., Rosenkranz, P. W., Smith, W. L., Staelin, D. H., et al.: AIRS/AMSU/HSB on the Aqua mission: Design, science objectives, data products, and processing systems, IEEE Transactions on Geoscience and Remote Sensing, 41, 253–264, 2003.
- 15 Bindoff, N. L., Stott, P. A., AchutaRao, M., Allen, M. R., Gillett, N., Gutzler, D., Hansingo, K., Hegerl, G., Hu, Y., Jain, S., et al.: Detection and attribution of climate change: from global to regional, 2013.
- Bleisch, R., Kämpfer, N., and Haefele, A.: Retrieval of tropospheric water vapour by using spectra of a 22 GHz radiometer, Atmospheric Measurement Techniques, 4, 1891–1903, doi:10.5194/amt-4-1891-2011, 2011.
- 20 Eriksson, P., Buehler, S., Davis, C., Emde, C., and Lemke, O.: ARTS, the atmospheric radiative transfer simulator, version 2, Journal of Quantitative Spectroscopy and Radiative Transfer, 112, 1551–1558, 2011.
- Flury, T., Hocke, K., Haefele, A., Kämpfer, N., and Lehmann, R.: Ozone depletion, water vapor increase, and PSC generation at midlatitudes by the 2008 major stratospheric warming, Journal of Geophysical Research: Atmospheres, 114, 2009.
- Haefele, A., De Wachter, E., Hocke, K., Kämpfer, N., Nedoluha, G., Gomez, R., Eriksson, P., Forkman, P., Lambert, A., and Schwartz, M.: 25 Validation of ground-based microwave radiometers at 22 GHz for stratospheric and mesospheric water vapor, Journal of Geophysical Research: Atmospheres, 114, 2009.
- Hauchecorne, A. and Chanin, M.-L.: Density and temperature profiles obtained by lidar between 35 and 70 km, Geophysical Research Letters, 7, 565–568, 1980.
- Keckhut, P., Wild, J. D., Gelman, M., Miller, A. J., and Hauchecorne, A.: Investigations on long-term temperature changes in the upper 30 stratosphere using lidar data and NCEP analyses, Journal of Geophysical Research: Atmospheres, 106, 7937–7944, 2001.
- Kunz, A., Pan, L., Konopka, P., Kinnison, D., and Tilmes, S.: Chemical and dynamical discontinuity at the extratropical tropopause based on START08 and WACCM analyses, Journal of Geophysical Research: Atmospheres, 116, 2011.
- Lamarque, J.-F., Emmons, L., Hess, P., Kinnison, D. E., Tilmes, S., Vitt, F., Heald, C., Holland, E. A., Lauritzen, P., Neu, J., et al.: CAM-chem: Description and evaluation of interactive atmospheric chemistry in the Community Earth System Model, Geoscientific Model 35 Development, 5, 369, 2012.
- Liebe, H., Hufford, G., and Cotton, M.: Propagation modeling of moist air and suspended water/ice particles at frequencies below 1000 GHz, in: In AGARD, Atmospheric Propagation Effects Through Natural and Man-Made Obscurants for Visible to MM-Wave Radiation 11 p (SEE N94-30495 08-32), vol. 1, 1993.
- Moreira, L., Hocke, K., Eckert, E., von Clarmann, T., and Kämpfer, N.: Trend analysis of the 20-year time series of stratospheric ozone profiles observed by the GROMOS microwave radiometer at Bern, Atmospheric Chemistry and Physics, 15, 10 999–11 009, 2015.
- Navas-Guzmán, F., Stähli, O., and Kämpfer, N.: An integrated approach toward the incorporation of clouds in the temperature retrievals from 5 microwave measurements, Atmospheric Measurement Techniques, 7, 1619–1628, 2014.
- Navas-Guzmán, F., Kämpfer, N., Murk, A., Larsson, R., Buehler, S., and Eriksson, P.: Zeeman effect in atmospheric O<sub>2</sub> measured by ground-based microwave radiometry, Atmospheric Measurement Techniques (AMT), 8, 1863–1874, 2015.
- Navas-Guzmán, F., Kämpfer, N., and Haefele, A.: Validation of brightness and physical temperature from two scanning microwave radiometers in the 60 GHz O<sub>2</sub>-band using radiosonde measurements, Atmospheric Measurement Techniques, 9, 4587–4600, 2016.

- 10 Ramaswamy, V. and Schwarzkopf, M.: Effects of ozone and well-mixed gases on annual-mean stratospheric temperature trends, *Geophysical research letters*, 29, 2002.
- Randel, W. J., Shine, K. P., Austin, J., Barnett, J., Claud, C., Gillett, N. P., Keckhut, P., Langematz, U., Lin, R., Long, C., et al.: An update of observed stratospheric temperature trends, *Journal of Geophysical Research: Atmospheres*, 114, 2009.
- 15 Remsberg, E., Lingenfelter, G., Harvey, V., Grose, W., Russell, J., Mlynczak, M., Gordley, L., and Marshall, B.: On the verification of the quality of SABER temperature, geopotential height, and wind fields by comparison with Met Office assimilated analyses, *Journal of Geophysical Research: Atmospheres*, 108, 2003.
- Rodgers, C. D.: *Inverse methods for atmospheric sounding: theory and practice*, vol. 2, World scientific, 2000.
- Rosenkranz, P.: *Absorption of microwaves by atmospheric gases*, 1993.
- Rosenkranz, P. W.: Water vapor microwave continuum absorption: A comparison of measurements and models, *Radio Science*, 33, 919–928, 20 1998.
- Santer, B., Penner, J., Thorne, P., Collins, W., Dixon, K., Delworth, T., Doutriaux, C., Folland, C., Forest, C., Hansen, J., et al.: How Well Can the Observed Vertical Temperature Changes be Reconciled with our Understanding of the Causes of These Temperature Changes?, 2006.
- Scheiben, D., Straub, C., Hocke, K., Forkman, P., and Kämpfer, N.: Observations of middle atmospheric H<sub>2</sub>O and O<sub>3</sub> during the 2010 major 25 sudden stratospheric warming by a network of microwave radiometers, *Atmospheric Chemistry and Physics*, 12, 7753–7765, 2012.
- Schwartz, M., Lambert, A., Manney, G., Read, W., Livesey, N., Froidevaux, L., Ao, C., Bernath, P., Boone, C., Cofield, R., et al.: Validation of the Aura Microwave Limb Sounder temperature and geopotential height measurements, *Journal of Geophysical Research: Atmospheres*, 113, 2008.
- Schwarzkopf, M. D. and Ramaswamy, V.: Evolution of stratospheric temperature in the 20th century, *Geophysical Research Letters*, 35, 30 2008.
- Shvetsov, A., Fedoseev, L., Karashtin, D., Bol'shakov, O., Mukhin, D., Skalyga, N., and Feigin, A.: Measurement of the middle-atmosphere temperature profile using a ground-based spectroradiometer facility, *Radiophysics and Quantum Electronics*, 53, 321–325, 2010.
- Stähli, O., Murk, A., Kämpfer, N., Mätzler, C., and Eriksson, P.: Microwave radiometer to retrieve temperature profiles from the surface to the stratopause, *Atmospheric Measurement Techniques*, 6, 2477–2494, 2013.
- 35 Steinbrecht, W., McGee, T., Twigg, L., Claude, H., Schönenborn, F., Sumnicht, G., and Silbert, D.: Intercomparison of stratospheric ozone and temperature profiles during the October 2005 Hohenpeißenberg Ozone Profiling Experiment (HOPE), *Atmospheric Measurement Techniques*, 2, 125–145, 2009.
- 645 Waters, J. W.: Ground-based measurement of millimetre-wavelength emission by upper stratospheric O<sub>2</sub>, *Nature*, 242, 506–508, 1973.
- Waters, J. W., Froidevaux, L., Harwood, R. S., Jarnot, R. F., Pickett, H. M., Read, W. G., Siegel, P. H., Cofield, R. E., Filipiak, M. J., Flower, D. A., et al.: The earth observing system microwave limb sounder (EOS MLS) on the Aura satellite, *IEEE Transactions on Geoscience and Remote Sensing*, 44, 1075–1092, 2006.
- Yan, X., Wright, J. S., Zheng, X., Livesey, N. J., Vömel, H., and Zhou, X.: Validation of Aura MLS retrievals of temperature, water vapour and 650 ozone in the upper troposphere and lower-middle stratosphere over the Tibetan Plateau during boreal summer, *Atmospheric Measurement Techniques*, 9, 3547, 2016.